

Macroscopic delayed-choice and retrocausality: quantum eraser, Leggett-Garg and dimension witness tests with cat states

Manushan Thenabadu and M. D. Reid¹

¹ *Centre for Quantum Science and Technologies Theory,
Swinburne University of Technology, Melbourne 3122, Australia*

We propose delayed choice experiments carried out with macroscopic qubits, realised as macroscopically-distinct coherent states $|\alpha\rangle$ and $|-\alpha\rangle$. Quantum superpositions of $|\alpha\rangle$ and $|-\alpha\rangle$ are created via a unitary interaction $U(\theta)$ based on a nonlinear Hamiltonian, in analogy with polarising beam splitters used in photonic experiments. Macroscopic delayed-choice experiments give a compelling reason to develop interpretations not allowing macroscopic retrocausality (MrC). We therefore consider weak macroscopic realism (wMR), which specifies a hidden variable λ_θ to determine the macroscopic qubit value (analogous to ‘which-way’ information), independent of any future measurement setting ϕ . Using entangled cat states, we demonstrate a quantum eraser where the choice to measure a which-way or wave-type property is delayed. Consistency with wMR is possible, if we interpret the macroscopic qubit value to be determined by λ_θ without specification of the state at the level of order \hbar , where fringes manifest. We then demonstrate violations of a delayed-choice Leggett-Garg inequality, and of the dimension witness inequality applied to the Wheeler-Chaves-Lemos-Pienaar experiment, where measurements need only distinguish the macroscopic qubit states. This negates all two-dimensional non-retrocausal models, thereby suggesting MrC. However, one can interpret consistently with wMR, thus avoiding conclusions of MrC, by noting extra dimensions, and by noting that the violations require further unitary dynamics U for each system. The violations are then explained as failure of deterministic macroscopic realism (dMR), which specifies validity of λ_θ *prior* to the dynamics $U(\theta)$ determining the measurement setting θ . Finally, although there is consistency with wMR for macroscopic observations, we demonstrate Einstein-Podolsky-Rosen-type paradoxes at a microscopic level, based on fringe distributions.

I. INTRODUCTION

Gedanken experiments in which there is a delayed choice of measurement motivated Wheeler and others to consider whether quantum mechanics implied a failure of realism, or else retrocausality [1–3]. The central argument has been presented for the two-slit experiment, in which a photon travels through the slits exhibiting either particle or wave-like behaviour. The observation of an interference pattern is interpreted as wave-like behaviour, while the observation that the photon travelled along a single path is interpreted as particle-like behaviour. A similar proposal exists for a Mach-Zehnder (MZ) interferometer, in which the photon travels in one or other path associated with the outputs of a beam splitter [1, 2]. In the delayed-choice quantum eraser [4], the decision to observe either the wave or particle-like behaviour is delayed until after the photon has passed through the apparatus, and the fringe distribution vanishes or emerges, conditionally on the measurement made at the later time. Thus there is an apparently paradoxical situation whereby it seems as though whether the photon went through “both slits” or “one slit” can be changed by an event (the choice of measurement) in the future.

Multiple different refinements and interpretations have been given [3, 5–28], but the consensus is that the original delayed-choice experiments do not imply the need for retrocausality. The above paradox arises only if one views the system as being either a wave or particle. The work of Ionicioiu and Terno proposed a quantum

beam splitter [19], which would place the system in a quantum superposition of wave- and particle-like states. An intermediate regime can be quantified, and a class of hidden variable theories based on the assumption of either wave- or particle-like behaviour can be negated [19, 20]. Significantly, Chaves, Lemos and Pienaar (CLP) resolved these issues further by explicitly constructing a two-dimensional causal model to explain the original MZ delayed-choice experiment [26], thus ruling out any need for retrocausal explanations.

On the other hand, with the inclusion of an additional phase shift in the MZ interferometer, CLP demonstrated that a two-dimensional classical model would need to be retrocausal to explain the predicted observations, which lead to a violation of a dimension witness inequality. Recent experiments confirm these predictions [27, 28]. In their analysis, the meaning of “non-retrocausal” is that, in a model which assumes realism, hidden variables λ associated with the preparation state are independent of any future measurement setting, ϕ . La Cour and Yudichak recently give a model which is nonretrocausal, but possesses extra dimensions [18]. Their model however is based on stochastic electrodynamics, which is not equivalent to quantum mechanics.

In this paper, we propose and analyse *macroscopic* versions of delayed-choice experiments. Our results demonstrate that delayed-choice paradoxes and the causal-modelling tests of CLP are evident at a macroscopic level, beyond \hbar , without the need for a microscopic resolution of measurement outcomes. Since retrocausality is more

paradoxical at a macroscopic level, we argue that this strengthens the need to explain the results of the experiments without invoking retrocausality.

Specifically, we follow [30–32] and map from a microscopic to a macroscopic regime, where spin qubits $|\uparrow\rangle$ and $|\downarrow\rangle$ are realised as macroscopically distinct coherent states $|\alpha\rangle$ and $|\alpha\rangle$ (α is large), that form a macroscopic qubit. The qubit values η of $+1$ and -1 corresponding to the coherent states $|\alpha\rangle$ and $|\alpha\rangle$ can be distinguished by a measurement of the field quadrature amplitude X , without the need to resolve at the level of \hbar . In analogy with a polarising beam splitter (PBS) used in the photonic experiments, superpositions of the two coherent states (called cat states) [29–32]

$$\cos\theta|\alpha\rangle + i\sin\theta|\alpha\rangle \quad (1)$$

can be created using a unitary interaction $U(t) \equiv U(\theta)$ based on a nonlinear Hamiltonian, H_{NL} . The value of t determines θ and hence the probability amplitudes of the two-state superposition. This provides a mechanism for a direct mapping from the microscopic to macroscopic delayed-choice experiments.

To analyse quantitatively, we seek to define *macroscopic retrocausality*. In analyses of the delayed-choice experiments, the meaning of retrocausality is intertwined with that of realism. Our approach is therefore closely linked to that of Leggett and Garg [33] and indeed we propose a delayed-choice version of the Leggett-Garg violation of macro-realism, showing violation of Leggett-Garg inequalities using cat states. Following Leggett and Garg, we define macroscopic realism: *Macroscopic realism* asserts a predetermination of the outcome for a measurement of the macroscopic qubit value η (the sign of X), for the system prepared at time t_M in a superposition (1). The variable λ_M describes the macroscopic state of the system at the time t_M and its value gives the outcome of the qubit measurement η . Since the value does not require a microscopic resolution, the validity of λ_M at the given time t_M is a *very weak* assumption, compared to the assumption of Bell’s local hidden-variable states $\{\lambda_i\}$ [34] which give a realistic description for any measurement, including those that are microscopically resolved. The cat-state analysis enables a clear distinction between the macroscopic hidden variable λ_M and the more general hidden-variable states $\{\lambda_i\}$.

However, recent work establishes the need to also carefully consider whether the unitary rotation $U(\theta)$ associated with the measurement setting θ has been performed (or not) prior to t_M . This leads to two definitions of macroscopic realism, one of which (deterministic macroscopic realism) can be falsified [31, 32]. Deterministic macroscopic realism (dMR) asserts a predetermination of outcomes, at a time t , for multiple future choices of θ (e.g. θ_1 and $\theta_2 = \phi$), so that these outcomes are given by multiple hidden variables (e.g. λ_{M1} and λ_{M2}) simultaneously specified at t .

To examine macroscopic retrocausality, we therefore consider *weak macroscopic realism* (wMR) [32]: Weak macroscopic realism asserts that the system prepared at time t_M in a superposition (1) is in a state giving a definite outcome λ_M (λ_M being $+1$ or -1) for the macroscopic pointer qubit measurement η . It is implicit as part of the definition that the value λ_M be independent of any future measurement setting, ϕ . We use the term *pointer measurement*, because it is assumed that the unitary rotation $U(\theta)$ determining the measurement setting has already been performed, *prior* to t_M i.e. the system has been prepared in the appropriate basis, θ .

In this paper, we examine the unitary dynamics $U(t)$, showing that at certain times t_M the assumption of λ_M is relevant, because the system is in a two-state superposition (1). During the dynamics, however, the state of the system has a more general form than (1). Extra dimensions are evident in the quantum continuous-variable phase-space representations for the system. Thus, it is possible to argue consistently with the Chaves-Lemos-Pienaar (CLP) analysis that λ_M is valid at the time t_M , and hence that there is no macroscopic retrocausality. Instead, the violations of the dimensions witness inequality and delayed-choice Leggett-Garg inequalities reflect the failure of dMR, which (it is argued) arises from failure of Bell-type hidden variables $\{\lambda_i\}$ defined microscopically.

In summary, the main results of this paper are two-fold: First, we demonstrate the possibility of performing macroscopic delayed-choice tests using cat states, including those of the type previously proposed at a microscopic level by CLP. Second, we explain how these predictions can be viewed consistently with wMR, thus providing a counter argument to any conclusions of macroscopic retrocausality. Lastly, although there is no inconsistency with wMR at a macroscopic level, we point out EPR-type paradoxes [32, 35] giving inconsistencies with the completeness of quantum mechanics at a microscopic level, where fringes in the distributions are evident.

II. SUMMARY OF PAPER

The paper is organised as follows. In section III, we consider a quantum eraser experiment. In analogy with experiments using entangled states [3, 7, 24], the system is prepared at $t_1 = 0$ in a two-mode entangled cat state $\sim |\alpha\rangle_a |\beta\rangle_b - |-\alpha\rangle_a |\beta\rangle_b$. We identify the qubit value η_i at time t_i as “which-way” information. The qubit value for a can be determined by a quadrature measurement X_B of the mode b , and the interference for system a created by interacting locally according to $U_A(t_2)$ for a specific time t_2 . Similarly, one may apply $U_B(t_2)$ for b . The loss of which-way information is identified by fringes in the distributions of the orthogonal quadrature P_A for a . However, we conclude there is no paradox involving macroscopic retrocausality, since the fringes are only dis-

tinguished at the level of \hbar . The results can be viewed consistently with weak macroscopic realism. Nonetheless, in Section VI we show that at the *microscopic* level of \hbar , EPR-type paradoxes can be constructed (similar to those discussed in [32, 36]), based on the fringe pattern.

We turn to macroscopic paradoxes, in Section IV, by presenting tests where it is only necessary to measure the macroscopic qubit value η . We show violation of a Leggett-Garg inequality, where one measures η_i at three times t_i ($t_3 > t_2 > t_1$). The violation reveals failure of the joint assumptions of *weak macroscopic realism* (wMR) and *noninvasive measurability* (called *macrorealism*). Noninvasive measurability asserts that one can determine the value of λ_i for the system satisfying wMR, in a way that does not affect the future λ_j ($j > i$). In the present proposal, the measurement of λ_i ($i = 1, 2$) of a is justified to be noninvasive because it is performed on the spacelike separated system b and, furthermore, the choice of which measurement (λ_1 or λ_2) to make is delayed, until after t_3 . A natural interpretation is that the measurement of λ_2 (or λ_1) disturbs the dynamics to affect the result for λ_3 , therefore violating macrorealism. Since there is a delayed choice, this suggests macroscopic retrocausality. In Section V, we follow the Chaves-Lemos-Pienaar experiment, demonstrating violation of the dimension witness inequality for cat states, thus falsifying all two-dimensional non-retrocausal models [26]. This consolidates the work of [32], which outlined the possibility of delayed-choice experiments with cat states.

To counter conclusions of macroscopic retrocausality, in Section IV.C we give an interpretation of the violations of the delayed-choice Leggett-Garg inequalities that is consistent with wMR: The apparent macroscopic retrocausality comes about because of the entanglement with the meter system b at the time t_2 , and the macroscopic nonlocality associated with the dynamics of the unitary rotations, when such rotations occur for *both* systems after the time t_2 . Using phase-space depictions of $P(X_A, X_B)$, we identify extra dimensions not present in the two-dimensional non-retrocausal models. We show that the violation of the Leggett-Garg inequalities certifies a failure of *deterministic macroscopic realism* (dMR), but not wMR (which is a weaker assumption than dMR). A similar explanation is given in Section V to explain the violation of the dimension witness inequality.

III. DELAYED-CHOICE QUANTUM ERASER WITH ENTANGLED CAT STATES

A. Set-up

We begin by presenting an analogue of the delayed-choice quantum eraser experiment, for cat states. We consider the variant that uses two spatially separated systems A and B . The overall system is prepared at time

$t_1 = 0$ in the entangled cat Bell state [37]

$$|\psi_{Bell}(t_1)\rangle = \mathcal{N}\{|\alpha\rangle|-\beta\rangle - |-\alpha\rangle|\beta\rangle\} \quad (2)$$

where $|\alpha\rangle$ and $|\beta\rangle$ are coherent states for single-mode systems A and B . We take α and β to be real, positive and large. Here, $\mathcal{N} = \frac{1}{\sqrt{2}}\{1 - \exp(-2|\alpha|^2 - 2|\beta|^2)\}^{-1/2}$ is the normalisation constant.

For each system, one may measure the field quadrature phase amplitudes $\hat{X}_A = \frac{1}{\sqrt{2}}(\hat{a} + \hat{a}^\dagger)$, $\hat{P}_A = \frac{1}{i\sqrt{2}}(\hat{a} - \hat{a}^\dagger)$, $\hat{X}_B = \frac{1}{\sqrt{2}}(\hat{b} + \hat{b}^\dagger)$ and $\hat{P}_B = \frac{1}{i\sqrt{2}}(\hat{b} - \hat{b}^\dagger)$, which are defined in a rotating frame, with units so that $\hbar = 1$ [29]. The boson destruction mode operators for modes A and B are denoted by \hat{a} and \hat{b} , respectively. The outcome X_A of the measurement \hat{X}_A distinguishes between the states $|\alpha\rangle$ and $|-\alpha\rangle$, and similarly \hat{X}_B distinguishes between the states $|\beta\rangle$ and $|-\beta\rangle$. We define the outcome of the measurement $\hat{S}^{(A)}$ to be $S^{(A)} = +1$ if $X_A > 0$, and -1 otherwise. Similarly, the outcome of the measurement $\hat{S}^{(B)}$ is $S^{(B)} = +1$ if $X_B > 0$, and -1 otherwise. S is identified as the spin of the system i.e. the qubit value η .

The coherent states of A and B become orthogonal in the limit of large α and β , in which case the superposition (2) maps onto the two-qubit Bell state

$$|\psi_{Bell}\rangle = \frac{1}{\sqrt{2}}(|+\rangle_a|-\rangle_b - |-\rangle_a|+\rangle_b) \quad (3)$$

At time t_1 , the outcomes for $S^{(A)}$ and $S^{(B)}$ are anti-correlated. Therefore, one may infer the outcome for $S^{(A)}$ noninvasively by measuring X_B , and hence $S^{(B)}$.

We present an analogy with the delayed-choice quantum eraser based on the photonic versions of the state (3). In the photonic version, the next step is that the photon of system A propagates through two slits, or else through a 50/50 beam splitter ($BS1$) with two equally probable output paths as in a Mach-Zehnder (MZ) interferometer. If a single photon is incident on $BS1$, this creates a superposition e.g. for mode A , the state $|+\rangle_a$ is transformed to

$$|\psi\rangle_{a,2} = \frac{1}{\sqrt{2}}(|+\rangle_{a,2} + i|-\rangle_{a,2}) \quad (4)$$

where $|+\rangle_{a,2}$ and $|-\rangle_{a,2}$ refer to the photon in paths designated $+$ or $-$ in the MZ interferometer. In the original quantum eraser, the measurement of which-way information is made by measuring whether the system is $+$ or $-$. This is done by recombining the paths using a second beam splitter $BS2$, which is set to be fully transmitting so that the paths are not mixed. An alternative choice is that $BS2$ is similar to $BS1$ with a 50% transmittivity, which restores the state $|+\rangle$, the photon appearing only at one of the output paths, indicating interference.

In the cat-state gedanken experiment, the superposition (4) is achieved by a unitary interaction $U(t)$ for a particular choice $t = t_3$. We consider $t_2 < t_3$ in the next

Section. After preparation at the time t_1 , the systems A and B evolve independently according to the local unitary transformations $U_A(t_a)$ and $U_B(t_b)$, defined by

$$U_A(t_a) = e^{-iH_{NL}^{(A)}t_a/\hbar}, \quad U_B(t_b) = e^{-iH_{NL}^{(B)}t_b/\hbar} \quad (5)$$

where

$$H_{NL}^{(A)} = \Omega \hat{n}_a^k, \quad H_{NL}^{(B)} = \Omega \hat{n}_b^k \quad (6)$$

Here t_a and t_b are the times of evolution at each site, k is a positive integer, $\hat{n}_a = \hat{a}^\dagger \hat{a}$ and $\hat{n}_b = \hat{b}^\dagger \hat{b}$, and Ω is a constant. We take $k = 2$; or else $k > 2$ and k is even. As the systems evolve, the spin for each can be measured at a given time. We denote the value of spin $S^{(A)}$ after an interaction time $t_a = t_i$ to be $S_i^{(A)}$, and the value of the spin $S^{(B)}$ after the interaction time $t_b = t_j$ to be $S_j^{(B)}$. The dynamics of the unitary evolution (5) is well known [29, 38, 39]. If the system A is prepared in a coherent state $|\alpha\rangle$, then after at time $t_a = t_3 = \pi/2\Omega$, the state of the system A is [30–32]

$$U_{\pi/4}^{(A)}|\alpha\rangle = e^{-i\pi/4}\{\cos \pi/4|\alpha\rangle + i \sin \pi/4|-\alpha\rangle\} \quad (7)$$

where $U_{\pi/4}^{(A)} = U_A(\pi/2\Omega)$. A similar transformation $U_{\pi/4}^{(B)}$ is defined at B for $t_b = t_3 = \pi/2\Omega$. We note the state (7) maps onto (4). The generation of the superposition (7) using $k = 2$ has been reported in [38, 39]. The system A in the superposition (7) exhibits interference fringes in the distribution $P(P_A)$ for \hat{P}_A [29].

According to the premise *weak macroscopic realism* (wMR) defined in the Introduction, at the time t_2 the system (7) may be regarded as being in one or other of two macroscopically distinguishable states (φ_+ and φ_-) which have a definite value $+1$ or -1 for the outcome $S_3^{(A)}$. While it might be tempting to identify the states φ_+ and φ_- as being $|\alpha\rangle$ and $|-\alpha\rangle$, this would be a full microscopic identification of the states in quantum terms. The states φ_+ and φ_- are not specified to this precision. The states φ_+ and φ_- correspond to distinct values of the *macroscopic* observable $S_3^{(A)}$ only. The determination of the value of $S_3^{(A)}$ gives the “which-way” information in the quantum eraser experiment. If one is able to design an appropriate macroscopic observable (similar to $S_3^{(A)}$) for the two-slit and MZ scenarios, then the assumption of wMR is analogous to the interpretation that the particle goes through one slit or the other in the double slit experiment, or goes through one path or the other, in the MZ interferometer. This assumption however, does *not* specify the system to be in *either* state $|+\rangle_{a,2}$ or $|-\rangle_{a,2}$.

If one evolves for a time of $t_3 = \pi/2\Omega$ at both sites, then the final state is

$$\begin{aligned} |\psi_{Bell}(t_3)\rangle &= U_{\pi/4}^{(A)}U_{\pi/4}^{(B)}|\psi_{Bell}(t_1)\rangle \\ &= \mathcal{N}e^{-i\pi/4}(|\alpha\rangle|-\beta\rangle - |-\alpha\rangle|\beta\rangle) \end{aligned} \quad (8)$$

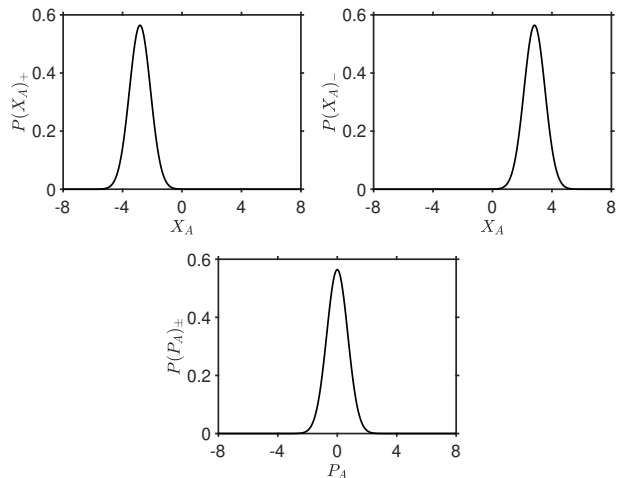


Figure 1. Top: Plots of $P(X_A)_\pm$ and $P(P_A)_\pm$ for the system A at time t_3 , when which-way information is present. The $P(P_A)_\pm$ show no fringes. Here, $\alpha = \beta = 2$.

which is a Bell state. At the time t_3 , the spin $S_3^{(A)}$ of system A can be inferred by measuring $S_3^{(B)}$, which is anticorrelated with the spin $S_3^{(A)}$ at A . This gives the which-way information of system A at time t_3 , analogous to measuring through which slit or path the photon went through in the original quantum eraser set-ups. Only the absolute interaction times t_a and t_b at each site are relevant to the correlation however, and it is hence possible to *delay* interaction at B until a time t_4 , after the system at A has already interacted.

With this method of measurement of $S_3^{(A)}$, the system A has not been directly measured. One can thus make a measurement of \hat{P}_A at the time t_3 . The system (being coupled to B) can be detected as being in one or other state, φ_+ or φ_- , giving $+$ or $-$ outcomes for $S_3^{(A)}$. Which-way information is present and, consistent with that, the distribution $P(P_A)$ shows no fringes. This is seen in Figure 1, where we plot the conditional distributions $P(X_A)_\pm$ and $P(P_A)_\pm$ given the outcome \pm for X_B at B , as evaluated from the joint distributions $P(X_A, X_B)$ and $P(P_A, X_B)$. The distribution $P(P_A)_\pm$ for an outcome P_A for the measurement \hat{P}_A is a Gaussian centred at 0 with no fringes present, consistent with that of the coherent state $|\pm\alpha\rangle$ [29].

On the other hand, one may take $t_a = t_3$ and $t_b = 0$, so that there is no local unitary interaction at B . Alternatively, one may evolve both sites according to $t_a = t_b = t_3$, and then perform a local unitary transformation $U_B(t_2)^{-1} = (U_{\pi/4}^{(B)})^{-1}$ at B , to transform the system B “back” to the initial state of B at time t_1 . Which-way information about A at t_3 is then absent. The state of the combined systems at this time $t_4 > t_3$ is

$$|\psi(t_4)\rangle = \mathcal{N}\{U_{\pi/4}^{(A)}|\alpha\rangle|-\beta\rangle - U_{\pi/4}^{(A)}|-\alpha\rangle|\beta\rangle\} \quad (9)$$

If the final stage of the spin measurement B is made at

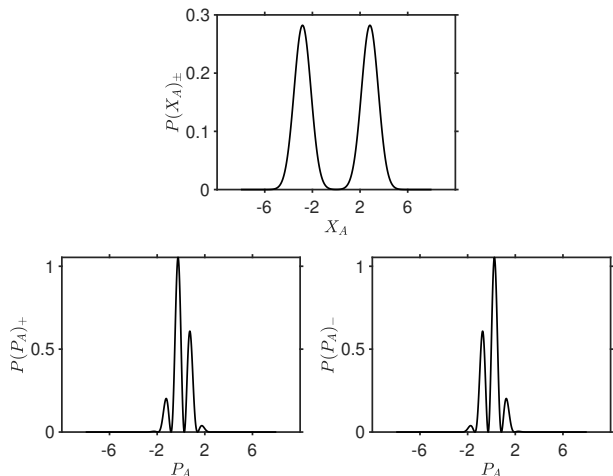


Figure 2. Top: Plots of $P(X_A)_\pm$ and $P(P_A)_\pm$ of the system A at time t_2 , where the outcome for $S_4^{(B)} = S_4^{(1)}$ is (left) $+1$, and (right) -1 . The which-way information is lost, and the system A is in the superposition (10). Here, $\alpha = \beta = 2$.

time t_4 , the result will give either $S^{(B)}(t_4) = 1$ or -1 . From the anti-correlation of (2), $S^{(B)}(t_4)$ is interpreted as a measurement of the initial value of $-S_1^{(A)}$, and hence knowledge of that state of system A at that time, t_1 . If the outcome of $S^{(B)}(t_4)$ is ∓ 1 then, assuming the limit where $|\beta\rangle$ and $|\alpha\rangle$ are orthogonal states (i.e. large β), the system A is projected into the superposition state

$$U_{\pi/4}|\pm\alpha\rangle = e^{-i\pi/4}\{\cos\pi/4|\pm\alpha\rangle + i\sin\pi/4|\mp\alpha\rangle\} \quad (10)$$

This is the state of the local system A at time t_2 (see eqn (7)), conditioned on the initial state of A at time t_1 being $|\pm\alpha\rangle$. Thus, if one measures $P(P_A)$ conditional on the result of $-S^{(B)}(t_4) = S_1^{(A)}$, the fringes are recovered. We find

$$P(P_A)_\pm = \frac{e^{-P_A^2}}{\sqrt{\pi}}\{1 \mp \sin(2\sqrt{2}P_A|\alpha|)\} \quad (11)$$

where $P(P_A)_+$ and $P(P_A)_-$ is the distribution for P_A conditional on the result $+1$ or -1 for $S_1^{(A)}$, respectively. The distributions (Figure 2) show fringes, indicative of the system A at time t_3 being in the superposition (10), and indicative of the loss of which-way information.

The accurate calculation of the conditional probabilities $P(P_A)_\pm$, without the simplistic assumption of a projection into a definite coherent state at A on measurement at B , gives

$$P(P_A)_\pm = \frac{2\mathcal{N}^2 e^{-P_A^2}}{\sqrt{\pi}} \left\{ 1 - e^{-2|\beta|^2} \cos(2\sqrt{2}P_A|\alpha|) \mp \sin(2\sqrt{2}P_A|\alpha|) \operatorname{erf}(\sqrt{2}|\beta|) \right\} \quad (12)$$

where erf is the error function. The plots are indistinguishable from those of the approximate result for $\beta > 1$,

the limit $\beta \rightarrow \infty$ being the limit of an ideal measurement. The calculations in Figures 1 and 2 are based on evaluation of the joint distribution $P(P_A, X_B)$ (refer to [31]).

B. Interpretation in terms of wMR

As summarised in the Introduction, the delayed choice experiment has been interpreted as suggesting retrocausality. The decision to observe either the particle-like behaviour (which-way information) or the wave-like behaviour (fringes) of system A is made at the later time t_4 (at B). This appears to retrospectively change the system A at time t_3 from being in “one or other state” (φ_1 or φ_2 ; $|\alpha\rangle$ or $|\beta\rangle$) to being “in both states” (since the observation of fringes in $P(P_A)$ is often interpreted to suggest the system A was in “both states”, $|\alpha\rangle$ and $|\beta\rangle$). As explained in [26], there is no requirement to assume retrocausality for the MZ delayed-choice experiment. The experiment described for cat states maps onto the qubit experiment for large α, β , and gives a similar conclusion for the macroscopic qubits.

The macroscopic version of the quantum eraser is informative, because with the introduction of the *macroscopic* hidden variable, λ_i , it allows us to separate the macroscopic from the microscopic behavior. We consider compatibility with the assumption of weak macroscopic realism (wMR) – that the system A at the time t_2 is in a state with a definite value $\lambda_3^{(A)}$ which corresponds to the outcome of a measurement $S_3^{(A)}$, should it be performed. Here, there is *no* attempt to define the *quantum* state associated with that predetermination, so that predictions for other more microscopic measurements (and hence other hidden variables that determine those predictions) are not relevant. Thus, wMR does not postulate that the system is in one or other state $|\alpha\rangle$ or $|\beta\rangle$. In fact, we see there is *no negation of wMR*, because the fringes are only evident at the microscopic level of \hbar (here $\hbar \sim 1$). The gedanken experiment is consistent with wMR. In that sense, the system always displays a particle-like behaviour.

The assumption of weak macroscopic realism (wMR) *if* applied to the double-slit experiment would be that the particle has a position constraining it to go through a definite slit even when fringes are observed (provided the slit does not restrict the position to of order \hbar or less). For the definition of wMR, the predictions for other more precise position or momentum measurements of order \hbar are not relevant. A similar interpretation of wMR for the MZ experiment is that the photon/particle takes one or other path with a macroscopic uncertainty, but is not defined to be in one or other state $|+\rangle_{a,2}$ and $|-\rangle_{a,2}$.

The interpretation based on wMR suggests a lack of completeness of the description at the microscopic level. This can be clarified further. Indeed, if wMR holds, then

it is possible to show that EPR-type paradoxes exist at the *microscopic* level. The EPR-type arguments indicate an *incompleteness* of a quantum state description if compatible with wMR, as explained in [32], and will be discussed further in Section VI.

IV. DELAYED-CHOICE LEGGETT-GARG TEST OF MACROREALISM

In this section, we consider the delayed choice experiment in the form of a Leggett-Garg test of macrorealism using entangled cat states. The advantage of the Leggett-Garg test is that all relevant measurements are macroscopic, distinguishing between the two macroscopically distinct coherent states. This contrasts with the quantum eraser proposal, where the paradoxical effects are inferred by the measurement of finely resolved fringes.

A. Set-up

At time t_1 , the system is prepared in the entangled cat state $|\psi_{Bell}(t_1)\rangle$ of eqn (2). The spatially separated systems A and B dynamically evolve according to the unitary interactions (5) where $k = 4$. We consider three times $t_1 = 0$, $t_2 = \pi/4\Omega$ and $t_3 = \pi/2\Omega$ (Figure 3). If the system at A were prepared in a coherent state $|\alpha\rangle$, then at the later time $t_a = t_2 = \pi/4\Omega$, the state of the system A at time t_2 is in the asymmetric superposition [30–32]

$$U_{\pi/8}^{(A)}|\alpha\rangle = e^{-i\pi/8}\{\cos\pi/8|\alpha\rangle + i\sin\pi/8|-\alpha\rangle\} \quad (13)$$

where $U_{\pi/8}^{(A)} = U_A(\pi/4\Omega)$. A similar transformation $U_{\pi/8}^{(B)}$ is defined at B for $t_b = t_2 = \pi/4\Omega$. If one evolves for a time of $t_2 = \pi/4\Omega$ at both sites, then the final state is

$$\begin{aligned} |\psi_{Bell}(t_2, t_2)\rangle &= U_{\pi/8}^{(A)}U_{\pi/8}^{(B)}|\psi_{Bell}(t_1)\rangle \\ &= \mathcal{N}e^{-i\pi/4}(|\alpha\rangle|-\beta\rangle - |-\alpha\rangle|\beta\rangle) \end{aligned} \quad (14)$$

The values of the macroscopic spins after the interaction time t_2 at each site are denoted $S_2^{(A)}$ and $S_2^{(B)}$. The spin $S_2^{(A)}$ of system A can be inferred by measuring $S_2^{(B)}$ which is anticorrelated with the spin at A .

On the other hand, one may choose to evolve at A for a time $t_a = t_2 = \pi/4\Omega$, but *not* at the site B , so that $t_b = 0$. The state after these interactions is

$$|\psi(t_2, t_1)\rangle = \mathcal{N}\{U_{\pi/8}^{(A)}|\alpha\rangle|-\beta\rangle - U_{\pi/8}^{(A)}|-\alpha\rangle|\beta\rangle\} \quad (15)$$

If the final readout stage of the spin measurement B is made at time t_4 (Figure 3), the result will give a value

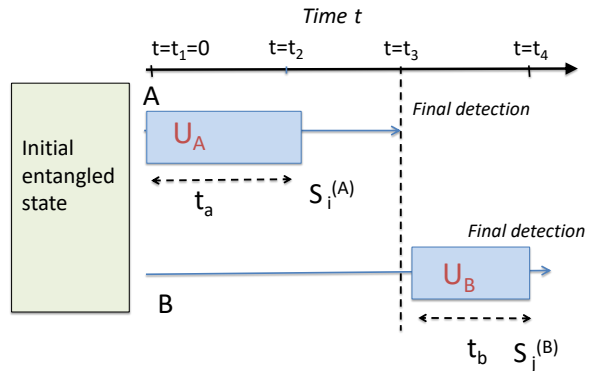


Figure 3. Sketch of the set-up for the delayed choice Leggett-Garg test. The system is prepared in the two-mode entangled cat state $|\psi_{Bell}(t_1)\rangle$ at the time $t_1 = 0$, with the modes spatially separated. Independent local unitary interactions U_A and U_B take place at sites A and B respectively, with time settings t_a and t_b . The times at A are selected as either $t_a = t_2 = \pi/4\Omega$ or $t_a = t_3 = \pi/2\Omega$ and the final detection enables measurement of $S_2^{(A)}$ or $S_3^{(A)}$ respectively. At B , one selects either $t_b = t_1 = 0$ or $t_b = t_2 = \pi/4\Omega$, the final detection enabling measurement of $S_1^{(B)}$ or $S_2^{(B)}$. The outcomes of $S_1^{(B)}$ and $S_2^{(B)}$ are anticorrelated with the outcomes of $S_1^{(A)}$ and $S_2^{(A)}$ respectively, if measured. In the delayed choice experiment, the interaction at B is delayed until after the final detection at A , at time t_3 . Hence, the measurement of $S_1^{(B)}$ (or $S_2^{(B)}$) allows inference of the past value of $S_1^{(A)}$ (or $S_2^{(A)}$).

$S^{(B)}(t_4) \equiv S_1^{(B)} = \pm 1$. From $|\psi_{Bell}(t_1)\rangle$ (eqn (2)), the value of $S^{(B)}(t_4)$ is anticorrelated with the initial value of $S_1^{(A)}$, if we had chosen $t_a = t_1 = 0$. Therefore the measurement at B is interpreted as a measurement of $S_1^{(A)}$. If the outcome of $S^{(B)}(t_4)$ is ∓ 1 then (assuming $|\beta\rangle$ and $|-\beta\rangle$ are orthogonal) from (9) we see that the system A is reduced to the superposition state

$$U_{\pi/8}|\pm\alpha\rangle = e^{-i\pi/8}\{\cos\pi/8|\pm\alpha\rangle + i\sin\pi/8|\mp\alpha\rangle\} \quad (16)$$

This is the state of the local system A at time t_2 (see eqn (7)), conditioned on the initial state of A at time t_1 being $|\pm\alpha\rangle$. The value of $S_2^{(A)}$ can be measured directly at A . This combination of interactions therefore allows measurement of both $S_2^{(A)}$ and $S_1^{(A)}$.

Alternatively, we may evolve the system A for a time $t_a = t_3 = \pi/2\Omega$, while not evolving at B ($t_b = t_1 = 0$). This gives

$$|\psi(t_3, t_1)\rangle = \mathcal{N}\{U_{\pi/4}^{(A)}|\alpha\rangle|-\beta\rangle - U_{\pi/4}^{(A)}|-\alpha\rangle|\beta\rangle\} \quad (17)$$

where $U_{\pi/4}|\pm\alpha\rangle$ is given by eqn (7). The spin $S_3^{(A)}$ can be measured directly at A . Measurement of $S^{(B)}(t_4) \equiv S_1^{(B)}$

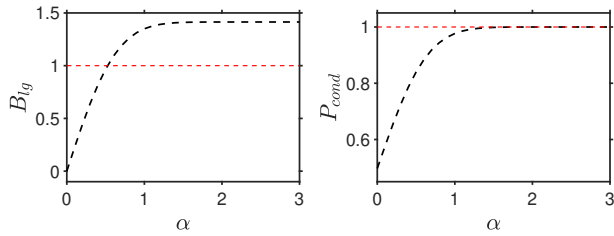


Figure 4. Violation of the Leggett-Garg inequality (18). We plot $B_{Lg} = -\{\langle S_1^{(B)} S_2^{(A)} \rangle - \langle S_1^{(B)} S_3^{(A)} \rangle + \langle S_2^{(B)} S_3^{(A)} \rangle\}$ versus α for the state $|\psi_{Bell}(t_1)\rangle$ (2), with $\beta = 2$. Violation is obtained when $B_{Lg} > 1$. The verification of $\langle S_i^{(A)} S_j^{(A)} \rangle = -\langle S_i^{(B)} S_j^{(A)} \rangle$ for $i = 1, 2$ is given by the conditional distribution P_{cond} defined as $P_{cond} = P(S_i^{(A)} = 1 | S_i^{(B)} = -1)$ as shown.

at B gives the inferred result for the measurement $S_1^{(A)}$. This allows measurement of both $S_3^{(A)}$ and $S_1^{(A)}$.

Alternatively, one may select $t_b = t_2 = \pi/4\Omega$ at B . According to (14), the measurement at B then allows measurement of $S_2^{(A)}$. If one evolves at A for a time $t_a = t_3 = \pi/2\Omega$, then this combination of interactions allows measurement of both $S_2^{(A)}$ and $S_3^{(A)}$.

The set-up (Figure 3) allows for a delayed choice of the measurement of either $S_1^{(A)}$ or $S_2^{(A)}$, by delaying the choice at B to measure either $S_1^{(B)}$ or $S_2^{(B)}$. This amounts to a delay in the choice to interact the system B for a time $t_b = 0$, or else to interact system B for a time $t_b = t_2$. This choice can be delayed until a time well after the time t_3 , and well after the final detection (given by the measurement and readout of X_A) takes place at A .

B. Leggett-Garg inequality and violations

We now summarise the Leggett-Garg test of macrorealism for this system [32]. The definition of macrorealism involves two assumptions: macroscopic realism and non-invasive measurability (NIM). For our purposes, we take the definition of macroscopic realism to be that of weak macroscopic realism (wMR) defined in the Introduction: This asserts that the system given by (1) is in a state with a definite prediction for the macroscopic spin $S^{(A)}$, $+1$ or -1 . The system can then be assigned the hidden variable λ , the value of λ being $+1$ or -1 , which determines the result of the measurement $S^{(A)}$ should it be performed. Macrorealism also implies NIM, that the value of λ can be measured with negligible affect on the subsequent macroscopic dynamics of the system.

For measurements of spin $S_j^{(A)}$ made on a single system A at consecutive times $t_1 < t_2 < t_3$, macrorealism implies the Leggett-Garg inequality [33, 40, 41]

$$B_{Lg} = \langle S_1^{(A)} S_2^{(A)} \rangle + \langle S_2^{(A)} S_3^{(A)} \rangle - \langle S_1^{(A)} S_3^{(A)} \rangle \leq 1 \quad (18)$$

As shown in [31, 32], the cat system of Section IV.A is

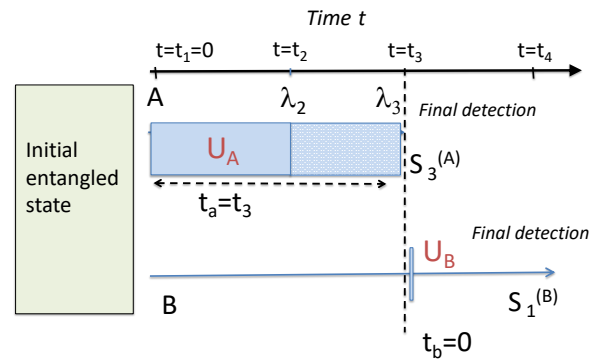
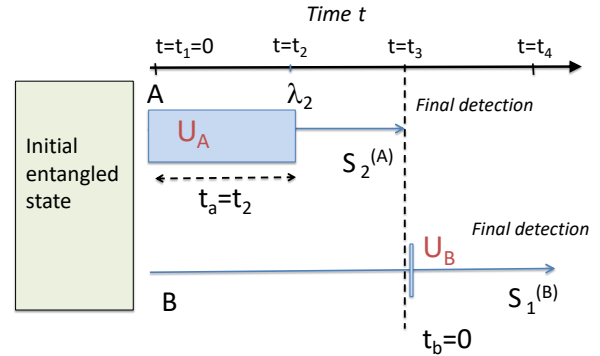


Figure 5. Sketch of the set-up for the delayed choice Leggett-Garg test. Notation is as for Figure 3. The top (lower) sketch shows measurement of $\langle S_2^{(A)} S_1^{(B)} \rangle$ ($\langle S_3^{(A)} S_1^{(B)} \rangle$). These measurements give the values of $\langle S_2^{(A)} S_1^{(A)} \rangle$ and $\langle S_3^{(A)} S_1^{(A)} \rangle$, based on the anticorrelation $S_1^{(B)} = -S_1^{(A)}$. For this measurement, there is no unitary interaction (rotation) at B . The predictions for the relevant distributions are given in Figure 7 (top). The results here are indistinguishable from those of an initial non-entangled state ρ_{mix} (compare Figure 8 (top)).

predicted to violate this inequality (Figure 4), meaning that macrorealism is falsified. While other Leggett-Garg inequalities have been proposed (e.g. [33, 42, 43]), this particular inequality is useful where measurements are made on entangled subsystems. The approach we give in this paper uses spatial separation *and* delayed-choice to justify noninvasiveness, since the measurements of $S_1^{(A)}$ and $S_2^{(A)}$ can be made on system B . The approach can be applied to other macroscopic superposition states, such as NOON states [44, 45] using the local unitary interaction given in [31]. We comment that violations of Leggett-Garg inequalities have been predicted and tested for a range of superposition states (e.g. [46–57]) and alternative procedures exist to justify NIM.

We summarise the measurements enabling a test of the

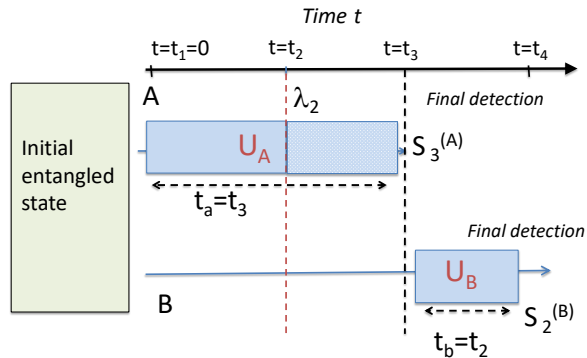


Figure 6. Sketch of the set-up for the Leggett-Garg test. Notation is as for Figure 3. The sketch depicts measurement of $\langle S_3^{(A)} S_2^{(B)} \rangle$, which based on the anticorrelation $S_2^{(B)} = -S_2^{(A)}$ gives the value for $\langle S_3^{(A)} S_2^{(A)} \rangle$. The predictions for the relevant distributions are given in Figure 7 (lower). The results at time t_4 are macroscopically different from those obtained if the state at time t_2 is non-entangled (compare Figure 8 (lower)). The results are inconsistent with local hidden variable models and the premise of deterministic macroscopic realism.

inequality (18), as in Figures 5 and 6. As we have seen, the value of $S_1^{(A)}$ or $S_2^{(A)}$ of system A can be inferred noninvasively by measurement of the anti-correlated spin $S_1^{(B)}$ or $S_2^{(B)}$. The result for the moment $\langle S_1^{(A)} S_2^{(A)} \rangle$ is determined by a direct measurement of $S_2^{(A)}$ at time t_2 , and an inferred measurement of $S_1^{(A)}$ by measuring $S_1^{(B)}$ at B (Figure 5). The moment $\langle S_1^{(A)} S_3^{(A)} \rangle$ is measured similarly (Figure 5).

The quantum prediction for $\langle S_1^{(A)} S_2^{(A)} \rangle$ is based on the assumption that the measurement of $S_1^{(B)}$ projects the system A into one or other state, $|\alpha\rangle$ or $|\beta\rangle$. The prediction is then $\langle S_1^{(A)} S_2^{(A)} \rangle = \cos(\pi/4)$, based on the evolution time of t_2 at A (see eqn (16)). The moment $\langle S_1^{(A)} S_3^{(A)} \rangle$ is evaluated similarly, and from eqn (7) we see the prediction is $\langle S_1^{(A)} S_3^{(A)} \rangle = \cos(\pi/2) = 0$.

For $\langle S_2^{(A)} S_3^{(A)} \rangle$, one would measure $S_2^{(B)}$ to determine the anticorrelated $S_2^{(A)}$, and measure $S_3^{(A)}$ directly at A (Figure 6). The prediction for $\langle S_2^{(A)} S_3^{(A)} \rangle$ is based on the assumption that the system A is in either $|\alpha\rangle$ or $|\beta\rangle$, at time t_2 (or else, that the measurement of $S_2^{(B)}$ projects A to one of these states). The subsequent evolution for a time $\Delta t = \pi/8$ then leads to the prediction of $\langle S_2^{(A)} S_3^{(A)} \rangle = \cos(\pi/4)$ (refer eqn (13)). This gives violation of the inequality (18), the left side being $\sqrt{2}$.

The above calculations assume large β (and hence orthogonal $|\beta\rangle$ and $|\alpha\rangle$) so that one may justify the assumption that the system A at times t_1 and t_2 is pro-

jected into one or other of the states $|\alpha\rangle$ or $|\beta\rangle$ once the measurement at B is performed. To evaluate accurately requires evaluation of the joint distributions $P(X_A, X_B)$ for the different times of interaction t_a and t_b . For large $\alpha, \beta > 1$. The precise results were calculated in [32], and are given in Figures 4. The results agree with the moments above, predicting violation of the inequality, for $\alpha > 1$. The plots of $P(X_A, X_B)$ for the various times of evolution are given in Figure 7.

The violation of the inequality (18) implies falsification of macrorealism. We note that the measurements $S_i^{(A)}$ and $S_j^{(B)}$ are macroscopic in the sense that one needs only to distinguish between the two macroscopically separated peaks of the distributions $P(X_A, X_B)$ (Figure 7). Here, the meaning of ‘‘macroscopic’’ refers to a separation in phase space of quadrature amplitudes X by an arbitrary amount ($\alpha \rightarrow \infty$).

C. Interpretation without macroscopic retrocausality

As explained above, macrorealism involves two assumptions: weak macroscopic realism (wMR) and noninvasive measurability. If we assume the validity of wMR, then we would conclude that noninvasive measurability fails: the measurement of the spin $S_i^{(B)}$ of B disturbs the result for the spin $S_j^{(A)}$ of A ($j > i$). However, since the measurements are made at B after the state of A at the time t_3 is measured, this conclusion would seem to suggest a macroscopic retrocausal effect, where which measurement is made at B alters the past value of λ_i at A . In Section IV, we rigorously clarify the nature of this apparent retrocausality, by examining the dimension witness test proposed in [26].

Here, we examine further, by analysing how the dynamics pictured in Figure 7 provides an interpretation that avoids the conclusion of macroscopic retrocausality. First, it is useful to compare with the dynamics of a non-entangled state (Figure 8)

$$\rho_{mix} = \frac{1}{2} \{ |\alpha\rangle\langle\alpha| - |\beta\rangle\langle\beta| + |\alpha\rangle\langle\beta| + |\beta\rangle\langle\alpha| \} \quad (19)$$

The non-entangled cat state is consistent with the first Leggett-Garg premise of weak macroscopic realism (wMR), since each system can be viewed as being in one or other of two macroscopically distinct coherent states at time t_1 . We first note that there is *no distinguishable difference* between the predictions $P(X_A, X_B)$ for the entangled ($|\psi_{Bell}(t_1)\rangle$) and non-entangled (ρ_{mix}) states, at the level of the macroscopic outcomes (compare the first plot of the top sequences in Figures 7 and 8). A distinction exists, but at order $\hbar e^{-|\alpha|^2}$, invisible on the plots.

It is seen that where one measures $S_1^{(B)}$, the predictions $P(X_A, X_B)$ for the two systems beginning with the

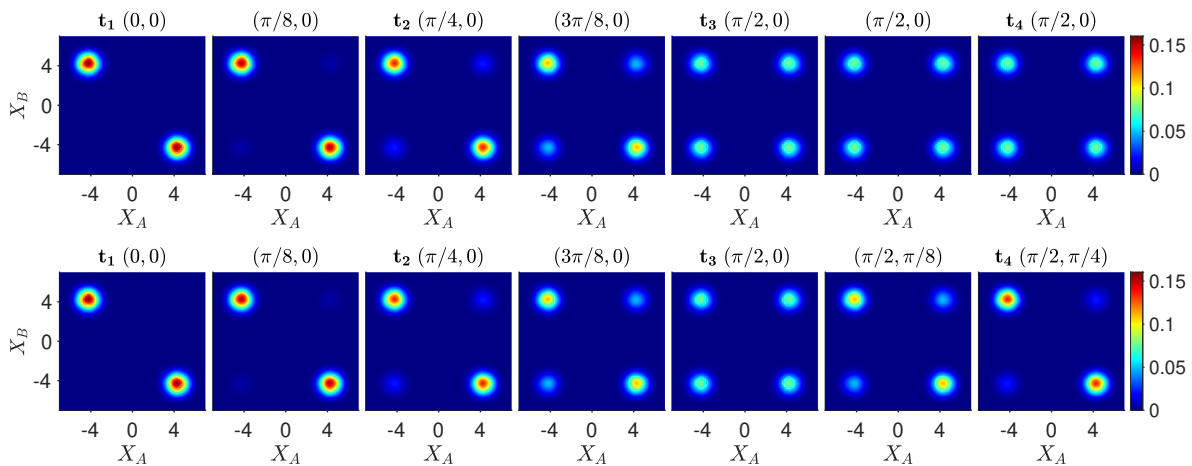


Figure 7. Contour plots of $P(X_A, X_B)$ showing the dynamics as the state $|\psi_{Bell}(t_1)\rangle$ evolves through the three measurement sequences of the Leggett-Garg test in the delayed-choice gedanken experiment depicted in Figures 5 and 6. Here, we go from time $t = t_1$ (far left), through to $t = t_2$ (third picture from left), $t = t_3$ (fifth picture from left) and, finally, $t = t_4$ (far right). The systems evolve locally according to $H_{NL}^{(A/B)}$ for interaction times t_a and t_b given by (t_a, t_b) in units of Ω^{-1} . Top: The sequence to infer $S_1^{(A)}$ by delayed measurement of $S_1^{(B)}$, enabling measurement of $\langle S_1^{(B)} S_3^{(A)} \rangle = -\langle S_1^{(A)} S_3^{(A)} \rangle$ (final picture), as in Figure 5 (lower). The sequence to measure $\langle S_1^{(B)} S_2^{(A)} \rangle = -\langle S_1^{(A)} S_2^{(A)} \rangle$ uses $t_a = t_2 = \pi/4$ as in Figure 5 (top) and ends with the third picture of the sequence. Lower: The sequence to infer $S_2^{(A)}$ by measurement of $S_2^{(B)}$, enabling measurement of $\langle S_2^{(B)} S_3^{(A)} \rangle = -\langle S_2^{(A)} S_3^{(A)} \rangle$ (final picture) as in Figure 6. Here, $t_1 = 0$, $t_2 = \pi/4$ and $t_3 = \pi/2$. $\alpha = \beta = 3$.

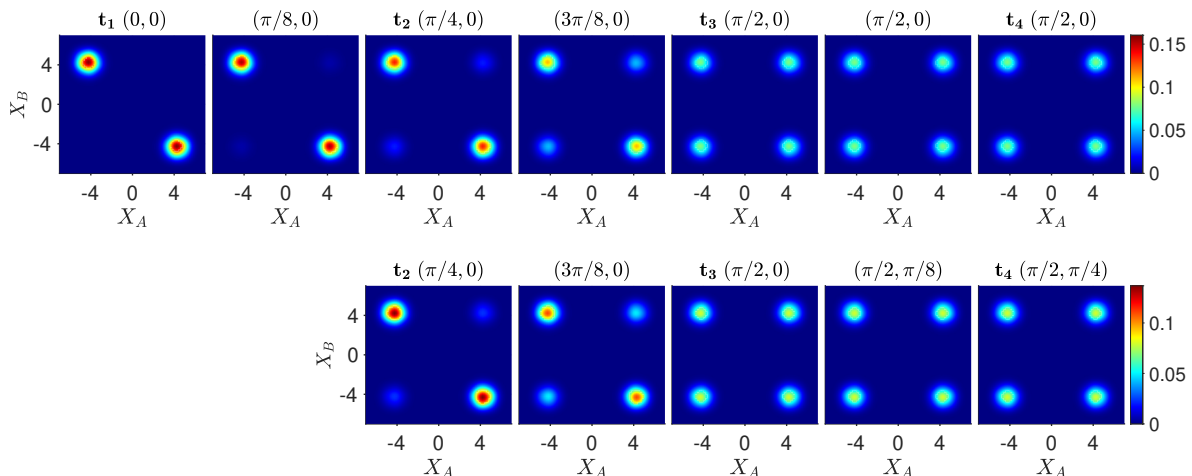


Figure 8. Contour plots of $P(X_A, X_B)$ showing the dynamics as the *non-entangled* state ρ_{mix} evolves through the same measurement sequences given in Figure 7. Notation as for Figure 7. Top: The sequence evolves as in Figure 5 (lower) with a unitary rotation at site A only. Although starting with ρ_{mix} at time t_1 , the sequence is indistinguishable from that given by the top sequence in Figure 7 for the entangled state $|\psi_{Bell}(t_1)\rangle$. Lower: We assume the system evolves as for Figure 6 and the lower sequence of Figure 7 with two unitary rotations, one at A and one at B , but starting from a nonentangled state ρ_{mix} at the time $t = t_2$. Although indistinguishable at the initial time t_2 , the final picture at $t = t_4$ ($(\pi/2, \pi/4)$) differs macroscopically from that of the entangled state (compare with the lower sequence in Figure 7).

entangled ($|\psi_{Bell}(t_1)\rangle$) and non-entangled (ρ_{mix}) states *remain indistinguishable* (compare the top sequences of Figures 7 and 8). This corresponds to there being no rotation (unitary evolution) at site B (Figure 5). A distinction in fact exists, but this is at the microscopic level of order $\hbar e^{-|\alpha|^2}$, invisible on the plots [32].

There is a *macroscopic* difference however for the evolution where one measures $S_2^{(B)}$, which involves *two* uni-

tary rotations after t_2 , one at each site, as depicted in Figure 6. This is seen by comparing the lower sequences of Figure 7 and Figure 8. Here, if one starts with a non-entangled state ρ_{mix} at time t_2 (Figure 8 (lower)), then even though the joint probabilities $P(X_A, X_B)$ are indistinguishable at t_2 , the joint probabilities differ macroscopically after the evolution involving rotations at both sites (compare the last pictures in the lower sequences).

We conclude that the violation of macrorealism and the apparent retrocausality arises from the measurement of $\langle S_2^{(A)} S_3^{(A)} \rangle$, as depicted in Figure 6. The scenario of Figure 5 is consistent with macrorealism, since it can be modelled by evolution of ρ_{mix} .

1. Weak macroscopic realism: the pointer measurement

To interpret without macroscopic retrocausality, we aim to show consistency with the assumption of weak macroscopic realism (wMR). We first examine this assumption more closely, along the lines given in [32].

Let us suppose the systems A and B are prepared at a time t_j in a macroscopic superposition $|\psi_{pointer}\rangle$ of states with definite outcomes for *pointer* measurements $\hat{S}_j^{(A)}$ and $\hat{S}_j^{(B)}$. In this paper, the example of such a superposition is

$$|\psi_{Bell}\rangle = \mathcal{N}(|\alpha\rangle|-\beta\rangle - |-\alpha\rangle|\beta\rangle) \quad (20)$$

where $\alpha, \beta \rightarrow \infty$. The premise wMR asserts that the system A at the time t_j is in one or other of two macroscopic states φ_+ and φ_- , for which the result of the spin measurement $S_j^{(A)}$ (given by the sign of the coherent amplitude) is determined to be $+1$ or -1 respectively. Hence, the system A at time t_j may be described by the macroscopic hidden variable $\lambda_j^{(A)}$. The value of $\lambda_j^{(A)}$ is fixed as either $+1$ or -1 at the particular time t_j , prior to the pointer measurement, and is independent of any future measurement. By the pointer measurement, it is meant that the measurement can be made as a final quadrature detection, X_A , with *no further unitary rotation* U_A necessary. Weak macroscopic realism does not mean that prior to the measurement of spin $S^{(A)}$ the system is in the state $|\alpha\rangle$ or $|-\alpha\rangle$, or indeed in any quantum state – since the quantum states are microscopically specified, giving predictions for all measurements that might be performed on A . For the entangled state $|\psi_{Bell}\rangle$, similar assumptions apply to system B .

For the bipartite system depicted in Figures 5 and 6, wMR is to be consistent with a form of macroscopic locality. “Macroscopic locality of the pointer” was summarised in [32] and asserts that the value of the macroscopic hidden variable $\lambda_j^{(A)}$ for the system A cannot be changed by any spacelike separated event, or measurement at the system B that takes place at time $t \geq t_j$ e.g. it cannot be changed by a future event at B . In this interpretation, the system A at each time t_i ($i = 1, 2, 3$) is in one or other of states $\varphi_{i,+}$ or $\varphi_{i,-}$ with a definite value $+1$ or -1 of spin $S_i^{(A)}$. The premise “macroscopic locality of the pointer” is to be distinguished from the stronger assumption, macroscopic locality, introduced in [32]. “Macroscopic locality” assumes locality to apply to spacelike-separated measurement events, but here the

measurement setting for system A is not necessarily established, so that A is *not necessarily prepared in the pointer basis*. This allows for the possibility of a further unitary rotation at A , before the final detection of X_A . The premise of weak macroscopic realism is thus not contradicted by the violation of the macroscopic Bell inequalities reported in [31, 32].

2. Delayed collapse and unitary rotation at one site only: consistency with wMR

The dynamics indicates consistency with wMR. We focus on two features, explained in Ref. [32]: delayed collapse and the single rotation.

Let us suppose that at the time t_j the dynamics $U^{(A)}$ for a pointer measurement $S_j^{(A)}$ has taken place at A . The final detection (the “collapse” or “projection”) stage of the measurement $S_j^{(A)}$ at A *can be delayed* for an infinite time, and there is no change in the *macroscopic* joint probabilities $P(X_A, X_B)$. The result is true even where there is a unitary rotation U_B at the site B after the time t_j : the joint probabilities $P(X_A, X_B)$ do not depend on whether the final detection at A is before or after the unitary evolution U_B . The full calculations are given in [32] and show that while there are differences in the final distributions, these differences are negligible, of order $\hbar e^{-|\alpha|^2}$. This supports the wMR assumption, that for the *pointer* measurement ($S_j^{(A)}$ in this case), the result is determined by $\lambda_j^{(A)}$ at the time t_j – we can consider $\lambda_j^{(A)}$ as fixed.

There is also consistency with wMR for the dynamics given by Figures 5 and 7 (top), where there is *no unitary rotation* at the site B (after t_1). Comparing Figures 7 (top) and 8 (top), we see that the macroscopic dynamics of the sequences for $\langle S_1^{(B)} S_3^{(A)} \rangle$ and $\langle S_1^{(B)} S_2^{(A)} \rangle$, which involve only one unitary rotation (at A), are identical to those of the non-entangled state ρ_{mix} , and hence are consistent with wMR. The macroscopic probabilities for the sequences with a rotation at one site only are also consistent with those of a local hidden variable theory i.e. the final outcomes at A and B can be interpreted as being due to a local interaction at A .

3. Failure of deterministic macroscopic realism: unitary rotation at both sites

The violations of the Leggett-Garg inequality can be shown to arise as a failure of deterministic macroscopic realism (dMR), as studied in [31, 32]. This premise (different to wMR) asserts a predetermined outcome for the measurement *prior* to the unitary rotation U that determines the measurement setting. Where one has *two* unitary rotations, one at each site, after the time t_j , as

in Figure 6, there is no longer consistency with the predictions of ρ_{mix} .

Let us consider the scenario of Figure 6, at time t_2 . The value of $\lambda_2^{(A)}$ is predetermined according to wMR, for the pointer measurement $S_2^{(A)}$. However, one may also consider the outcome of a measurement $S_3^{(A)}$ at the later time, made by applying a rotation $U^{(A)}(\pi/4)$ and then measuring X_A . If we assume dMR, then this latter outcome can also be regarded as predetermined, and we can assign the hidden variable $\lambda_3^{(A)}$ to the system at the time t_2 . Similarly, assuming dMR, one may assign variables $\lambda_2^{(B)}$ and $\lambda_3^{(B)}$ to system B , at time t_2 .

Extending this argument, the premise dMR would imply simultaneous values for the outcomes at time t_1 regardless of the future unitary dynamics required to make the actual measurements, and would hence imply the Leggett-Garg inequality (18). Similarly, the macroscopic Bell inequality studied in [31, 32] would apply. We have shown in Section IV.B that the Leggett-Garg inequality is violated, indicating failure of dMR. Similarly, the macroscopic Bell inequality derived in [31, 32] is violated. This implies that dMR is (predicted to be) falsified.

4. Explanation

The apparent retrocausal effect can be explained as arising from the failure of deterministic macroscopic realism. The failure of dMR may also be viewed as a macroscopic Bell nonlocality, as discussed in [31, 32]. We argue however that the gedanken experiment is consistent with weak macroscopic realism.

We explain further. First, examining Figure 7 for the Leggett-Garg violations, we see that the macroscopic dynamics of the sequences for $\langle S_1^{(B)} S_3^{(A)} \rangle$ and $\langle S_1^{(B)} S_2^{(A)} \rangle$ (Figure 5) involving only one unitary rotation are identical to those of the non-entangled state ρ_{mix} , and hence are consistent with wMR. We next consider measurement of $\langle S_2^{(A)} S_3^{(A)} \rangle$. In measuring $\langle S_2^{(A)} S_3^{(A)} \rangle$ via $\langle S_2^{(B)} S_3^{(A)} \rangle$, as in the lower sequence of Figure 7, the system at A is *entangled* with B at time t_2 . An interpretation consistent with wMR is possible, since the measurement of $\langle S_2^{(B)} S_3^{(A)} \rangle$ involves *two* rotations after the time t_2 , one at A and one at B (as in Figure 6). This double rotation gives rise to *macroscopic nonlocality* (violations of a macroscopic Bell inequality) i.e. to the failure of deterministic macroscopic realism [31, 32].

The validity of weak macroscopic realism can then be argued as follows (Figure 9). Following Figure 6, the system A at times t_1 and t_2 can indeed be represented by the hidden variables $\lambda_1^{(A)}$ and $\lambda_2^{(A)}$ (meaning that the pointer measurements of $S_1^{(A)}$ and $S_2^{(A)}$ have predetermined outcomes), because the predictions for pointer measurement $S_1^{(A)}$ and $S_2^{(A)}$ are identical with those arising from ρ_{mix}

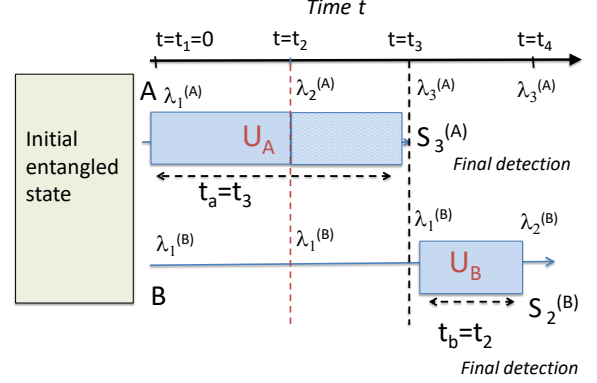


Figure 9. Consistency with weak macroscopic realism is possible for the time sequence of Figure 6. The system at time t_1 has valid hidden variables $\lambda_1^{(A)}$ and $\lambda_1^{(B)}$, being indistinguishable from ρ_{mix} . At time t_2 , system A has valid $\lambda_2^{(A)}$ and $\lambda_1^{(A)}$, the value of $\lambda_1^{(A)}$ being given by the pointer measurement on B at the time t_2 . Similarly, system B at time t_2 has valid $\lambda_1^{(B)}$ and $\lambda_2^{(B)}$. At time t_3 , the system A has valid $\lambda_3^{(A)}$ and $\lambda_1^{(A)}$, since the value of $\lambda_1^{(A)}$ can be given by the pointer measurement at t_3 on B . At time t_3 , system B has valid $\lambda_1^{(B)}$ and $\lambda_3^{(B)}$ (because $\lambda_3^{(B)}$ can be inferred from $\lambda_3^{(A)}$). At time t_4 , system A has valid $\lambda_3^{(A)}$ and $\lambda_2^{(A)}$.

(there has been a rotation at one site, A , only). This is also true of the system B at time t_1 : it can be described by a $\lambda_1^{(B)}$, for the reason that the predictions are indistinguishable from those of ρ_{mix} .

At time t_2 , A can also be consistently represented by a hidden variable $\lambda_1^{(A)}$, because the value $S_1^{(B)}$ at B is determinable by a pointer measurement, without further rotation. Also, because of the correlation with $S_2^{(A)}$, one would conclude $\lambda_2^{(B)}$ can be assigned to the state B at the time t_2 , because the outcome after the unitary evolution $U^{(B)}(\pi/4)$ is predetermined. However, it is *not* the case that at time t_2 the outcome of $S_3^{(A)}$ is predetermined (if $U^{(A)}(\pi/4)$ would be performed), because dMR fails. Hence, at time t_2 , it is not true that the hidden variable λ_3 can be assigned to the state at A , because the unitary rotation $U^{(A)}(\pi/4)$ has not been performed. Regardless, this does not imply failure of wMR, because the dynamics associated with $U^{(A)}(\pi/4)$ is in the future of t_2 .

On the other hand, if the unitary rotation $U^{(B)}(\pi/2)$ that precedes the measurement $S_3^{(B)}$ is performed *prior* to the time t_2 at B , then the state at A at time t_2 can be assigned $\lambda_3^{(A)}$, but can no longer be assigned $\lambda_1^{(A)}$ at that time t_2 . This interpretation allows for macroscopic Bell nonlocal effects when there are unitary rotations at both sites, but is also consistent with weak macroscopic realism (wMR) and hence does not indicate macroscopic retrocausality.

V. DIMENSION WITNESS TEST

We next follow the approach of Chaves, Lemos and Pienaar (CLP) [26], by demonstrating violation of the dimension witness inequality [27, 58–62]. Here, one considers two-dimensional models and, within this framework, confirms the failure of all non-retrocausal models. Our results extend beyond those of CLP because the conclusions of retrocausality apply to the macroscopic qubits $|\alpha\rangle$ and $|\alpha\rangle$ where α is large, for which the binary outcomes of the relevant measurements are distinguishable beyond \hbar . This test makes concrete the apparent retrocausality discussed in Section IV.C, and elucidates how this can be interpreted as due to the limitation of the assumption of two-dimensional hidden variable model.

We first consider the Wheeler-CLP delayed-choice experiment performed with tunable beam splitters i.e. with a variable reflectivity. A single boson is incident on the beam splitter, so that the input system is the two-mode state $|1\rangle_a|0\rangle_b$ (Figure 10). The two modes (c and d) at the outputs of the beam splitter have boson operators

$$\begin{aligned}\hat{c} &= \hat{a} \cos \theta - \hat{b} \sin \theta \\ \hat{d} &= \hat{a} \sin \theta + \hat{b} \cos \theta\end{aligned}\quad (21)$$

After the beam splitter, the state of the field in the interferometer is

$$|\psi\rangle_p = a^\dagger|0\rangle_a|0\rangle_b = \cos \theta|1\rangle_c|0\rangle_d + \sin \theta|0\rangle_c|1\rangle_d \quad (22)$$

This is the preparation state, prepared at time t_1 . The fields pass through the interferometer, and are recombined at a second beam splitter to produce final output modes e and f . The beam splitter transformation

$$\begin{aligned}\hat{e} &= \hat{c} \cos \phi - \hat{d} \sin \phi \\ \hat{f} &= \hat{c} \sin \phi + \hat{d} \cos \phi\end{aligned}\quad (23)$$

constitutes the measurement, and gives the final state

$$|\psi\rangle_m = \cos(\theta - \phi)|1\rangle_e|0\rangle_f + \sin(\theta - \phi)|0\rangle_e|1\rangle_f \quad (24)$$

The binary outcomes $|1\rangle_c|0\rangle_d$ and $|0\rangle_c|1\rangle_d$ are denoted $b = 1$ and $b = -1$ respectively. The expectation value for b is $E(\theta, \phi) = \cos^2(\theta - \phi) - \sin^2(\theta - \phi) = \cos(2(\theta - \phi))$. Certain choices of angles θ and ϕ will violate the dimension witness inequality, as we show below.

We map the above scheme onto a macroscopic system using the cat-state dynamics as shown by Figure 11. The input state is $|\alpha\rangle$. The nonlinear interaction H_{NL} replaces the beam splitter, and for certain choices of interaction time $t_\theta = m\pi/8$ where m is an integer prepares the system in the superposition

$$|\psi\rangle_p = e^{-i\varphi}(\cos \theta|\alpha\rangle + i \sin \theta|-\alpha\rangle) \quad (25)$$

where $\theta = t_\theta/2$ and $\varphi = t_\theta/2$ is a phase factor. This is proved in the Appendix C. The measurement stage

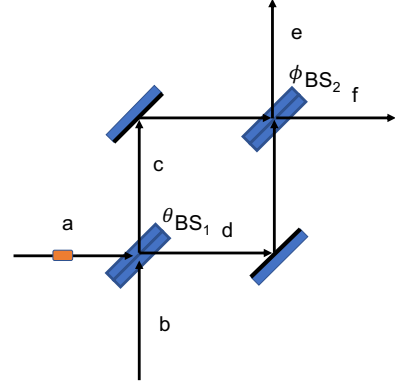


Figure 10. Schematic of Wheeler-CLP delayed choice experiment. A single boson two-mode state $|1\rangle_a|0\rangle_b$ is incident on the first beam splitter (BS_1). The first beam splitter introduces a variable reflectivity given by θ with output modes c and d . These two modes are again recombined at a second beam splitter BS_2 to produce final output modes e and f with variable transformation angle ϕ .

corresponding to the second beam splitter consists of a second interaction H_{NL} applied for a time t_ϕ , so that

$$|\alpha\rangle \rightarrow |\alpha\rangle_t = e^{-i\varphi_2}(\cos \phi|\alpha\rangle + i \sin \phi|-\alpha\rangle)$$

$$|-\alpha\rangle \rightarrow |-\alpha\rangle_t = e^{-i\varphi_2}(\cos \phi|-\alpha\rangle + i \sin \phi|\alpha\rangle) \quad (26)$$

for certain choices of ϕ . The final state after the interaction is

$$\begin{aligned}|\psi\rangle_f &= e^{-iH_{NL}t_\phi/\hbar}|\psi\rangle_p \\ &= e^{-i(\varphi+\varphi_2)}(\cos \theta(\cos \phi|\alpha\rangle + i \sin \phi|-\alpha\rangle) \\ &\quad + i \sin \theta(\cos \phi|-\alpha\rangle + i \sin \phi|\alpha\rangle)) \\ &= e^{i\eta}(\cos(\theta + \phi)|\alpha\rangle + i \sin(\theta + \phi)|-\alpha\rangle)\end{aligned}\quad (27)$$

where η is a phase factor. Identifying $b = 1$ as outcome $|\alpha\rangle$ and $b = -1$ as outcome $|-\alpha\rangle$, we obtain the results

$$E(\theta, \phi) = \cos(2(\theta + \phi)) \quad (28)$$

similar to the modified Wheeler-CLP delayed choice experiment. It is emphasized that the expression for $E(\theta, \phi)$ is only true for certain values of θ and ϕ , where (26) holds.

The set-up is an example of a prepare and measure scenario considered by CLP [26]. In their notation, the first measurement setting t_θ is denoted θ and the second t_ϕ is denoted by ϕ . They derived a dimension witness inequality (DWI) that is satisfied for nonretrocausal models of no more than two dimensions. In our notation, this inequality for the preparation settings $\theta, \theta', \theta''$ and the measurement settings ϕ, ϕ' is

$$\begin{aligned}I_{DW} &= \left| E(\theta, \phi) + E(\theta, \phi') + E(\theta', \phi) \right. \\ &\quad \left. - E(\theta', \phi') - E(\theta'', \phi) \right| \leq 3\end{aligned}\quad (29)$$

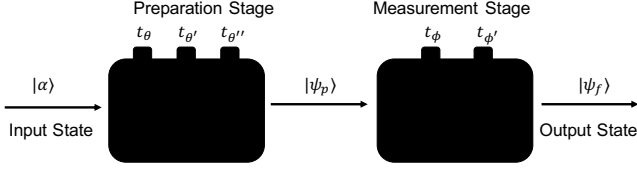


Figure 11. The set up for a macroscopic Wheeler-CLP delayed-choice experiment where we make use of the cat-state dynamics for a prepare and measure scenario. An initial input of $|\alpha\rangle$ undergoes a nonlinear interaction H_{NL} for a time t_θ at the preparation stage of the system corresponding to the first beam splitter $BS1$. A second interaction H_{NL} is applied for a time t_ϕ at the measurement stage which corresponds to the second beam splitter $BS2$. We make use of a dimension test on the final output to demonstrate failure of two-dimensional non-retrocausal models for the macroscopic system.

where here $E(\theta, \phi) = \cos(2(\theta + \phi))$. The t_θ and t_ϕ denote the time settings at the respective beam splitter interactions H_{NL} . If we violate DWI, then this indicates failure of all non-retrocausal classical two-dimensional models, suggesting the implication of retrocausality if we are to view the system as observing a two-dimensional classical realist model. For a classical two-dimensional model, one would conclude that the choice of measurement ϕ affects the earlier state.

The inequality DWI (29) also follows from the assumptions of macrorealism. Let us suppose the system to be in one or other of two states φ_+ and φ_- (such as $|\alpha\rangle$ and $|\alpha\rangle$) that will give outcomes $+1$ and -1 for the measurement of the macroscopic value S at the times t_p and t_m . Here, S is the sign of X_A , as defined in Sections III and IV. Then one may assign hidden variables $\lambda_p = \pm 1$ and $\lambda_m = \pm 1$ to the system at each of these times, the value $+1$ (-1) denoting that the outcome for S will be $+1$ (-1) respectively. If we assume one may measure the value of λ_p without affecting the value of λ_m at the later time (and vice versa), then the expectation value defined as $E(\theta, \phi) = \langle \lambda_p \lambda_m \rangle$ will satisfy the DW inequality. This is readily proved by calculating the averages allowing for all possible combinations of values ± 1 for λ_p and λ_m .

It is known that for the solution $E(\theta, \phi) = \cos(2(\theta - \phi))$ given by eq. (28), violation of the DW inequality is possible, the maximum value for I_{DW} being $I_{DW} = 1 + 2\sqrt{2} = 3.8284$. The angle choices are $\theta = \pi/8$, $\theta' = 3\pi/8$, $\theta'' = -\pi/4$, $\phi = \pi/4$, $\phi' = 0$ [26]. In the macroscopic case where the solution is $E(\theta, \phi) = \cos(2(\theta + \phi))$, we select $\theta = \pi/8$, $\theta' = 3\pi/8$, $\theta'' = 7\pi/4$, $\phi = 7\pi/4$, $\phi' = 0$. For these angle choices, the two-state solution (26) holds (refer Appendix C), as necessary for a macroscopic two-state test. The maximum violation $I_{DW} = 1 + 2\sqrt{2}$ is possible for this angle choice. We may also select $\theta = \pi/4$, $\theta' = \pi/2$, $\theta'' = 7\pi/8$, $\phi = 13\pi/8$, $\phi' = 15\pi/8$.

In Figure 12, we plot the Q function for the state of the system at the times t_0 , t_p and t_m . The Q function is

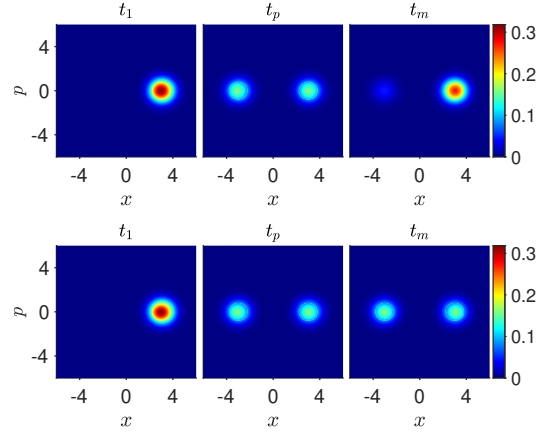


Figure 12. Contour plots for the Q function $Q(x, p)$ as the system of Figure 11 evolves from the coherent state $|\alpha\rangle$ at time $t_1 = 0$. (Top) In this sequence, the first interaction H_{NL} acts for a time $t_2 = t_\theta$, preparing the system in the two-state superposition $|\psi\rangle_p$ (eq. (25)) at the time $t_2 = t_p$. This is followed by a second interaction H_{NL} for a time t_ϕ to produce a final state at time $t_3 = t_m$. Here, $\theta = \pi/4$ and $\phi = -\pi/8$. (Lower) The lower sequence depicts the system prepared at the time t_p in a mixture of states $|\alpha\rangle$ and $|\alpha\rangle$. This occurs if the system is measured at that time, in such a way that the system collapses to the mixture. The system then evolves according to H_{NL} for a time t_ϕ to produce the final state at time $t_3 = t_m$.

defined as

$$Q(x, p) = \frac{1}{\pi} \langle \alpha_0 | \rho | \alpha_0 \rangle \quad (30)$$

where $|\alpha_0\rangle$ is a coherent state, and $\alpha_0 = x + ip$. The two-state dynamics is evident, as the system evolves under the action of H_{NL} . The H_{NL} provides the rotation into the superposition state, in analogy to the beam splitter interaction. Also plotted in Figure 12 is the Q function where the system at the time t_p is prepared in a mixture of $|\alpha\rangle$ and $|\alpha\rangle$. This applies where the system in the superposition at t_p is measured, so that an experimentalist may determine which of the states the system was in at the time t_p . In fact, the Q function for the superposition (top graph) differs from that of the mixture (lower graph) by terms of order $e^{-|\alpha|^2}$. For $\alpha > 1$, this difference is not visually noticeable on the scale of the plots. It is noted however that after the subsequent rotation H_{NL}^ϕ ($\phi \neq 0$), the Q functions provided from the superposition (top graph at time t_m) and the mixture (lower graph at t_m) are *macroscopically* distinguishable.

The Q function $Q(x, p)$ corresponds to anti-normally ordered moments, and hence does not directly correspond to the measured probabilities for x and p at the microscopic level of \hbar . However, at the macroscopic level where one distinguishes between the two states $|\alpha\rangle$ and $|\alpha\rangle$, the Q function accurately depicts the relative probabilities i.e. the weighting of the two peaks as pictured in the plots corresponds to the relative probabilities for the

binary outcomes, $b = 1$ and $b = -1$. The extra terms of order $e^{-|\alpha|^2}$ are negligible.

The violation of the dimension witness inequality indicates failure of two-dimensional non-retrocausal models. This is not inconsistent with the non-retrocausal interpretation given by Section IV.C, because the phase space dynamics relies on a *continuum* of values for X and P . At time t_2 there is no distinction between the *macroscopic* depictions $Q(x, p)$ for the superposition and mixed state (compare also the pictures at t_2 for the lower sequences of Figures 7 and 8). Yet, there are differences of order $\hbar e^{-|\alpha|^2}$. It is due to these *microscopic* differences between the superposition (entangled) and mixed (non-entangled) states, evident in the full phase-space distribution at t_2 , that there is a different dynamics, leading to a macroscopic difference in $E(\theta, \phi)$ at the later time t_3 .

VI. WEAK MACROSCOPIC REALISM AND EPR PARADOXES AT A MICROSCOPIC LEVEL

In the previous sections, we show how to realise macroscopic paradoxes involving Leggett-Garg and dimension witness inequalities. While there is a contradiction between deterministic macroscopic realism (dMR) and quantum mechanics for these paradoxes, inconsistency with weak macroscopic realism (wMR) is not demonstrated at this macroscopic level. However, inconsistencies arise at the microscopic level.

In this section, we show that at a *microscopic* level where measurements resolve at the level of \hbar , the premises of wMR and local causality give EPR-type paradoxes [35]. This implies that there is inconsistency between each of these premises and the *completeness* of quantum mechanics. EPR paradoxes involving local causality have been illustrated previously for macroscopic superpositions of type [63, 64]

$$|\psi\rangle = \frac{1}{\sqrt{2}}(|\alpha\rangle|\uparrow\rangle + |-\alpha\rangle|\downarrow\rangle) \quad (31)$$

often taken as an example of a ‘‘Schrodinger cat’’ state [65–67]. The approach here is similar, since for large β , the coherent states $|\beta\rangle$ and $|-\beta\rangle$ are orthogonal qubits.

A. EPR paradox using local causality

We consider the bipartite system prepared in the Bell state

$$|\psi_{Bell}\rangle = \frac{1}{\sqrt{2}}(|\alpha\rangle|-\beta\rangle - |-\beta\rangle|\alpha\rangle) \quad (32)$$

at time t_2 , as for (8). The original EPR argument shows incompatibility between the premise of local realism and the completeness of quantum mechanics [35]. The EPR

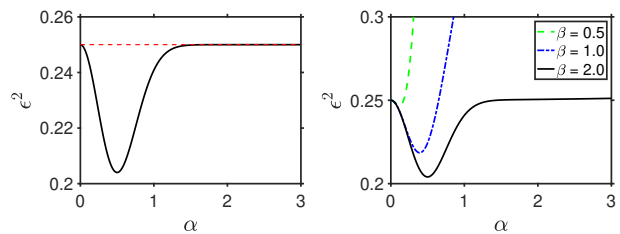


Figure 13. Plots showing the violation of the macroscopic EPR inequality (34). We first plot (left) \mathcal{E}^2 given by eqn (33). The same result is given for \mathcal{E}_M^2 which defined the macroscopic paradox, eq. (37). The second plot (right) shows the full calculation for \mathcal{E}^2 given by eqs. (35) and (36) based on the proposed method to measure β using X_B , which assumes β to be sufficiently large. Here, we show \mathcal{E}^2 versus α for $\beta = 0.5$, $\beta = 1$ and $\beta = 2$.

argument was generalised to allow for imperfect correlation between the two sites in [68], including for spin systems in [69, 70]. Here, we apply this generalisation to illustrate the paradox for the entangled Bell cat state.

The EPR argument considers the prediction for X_A , given a measurement at B . A measurement of $S_2^{(B)}$ at B will ‘‘collapse’’ system A to the quantum state $|\alpha\rangle$ or $|-\alpha\rangle$, implying a variance $(\Delta X_A)^2 = 1/2$ for A , conditioned on the result for $S_2^{(B)}$. We write this conditional variance as $\Delta_{inf}^2 X_A \equiv (\Delta_{inf} X_A)^2 = 1/2$, the variance for the inference of X_A given the measurement at B .

The EPR argument then considers the prediction for P_A of system A at time t_2 , as can be inferred from a measurement made at B . Here, we propose that the measurement made at B be given by $U_B(t_2)^{-1}$ followed by a measurement of $S_2^{(B)}$ (the sign of \hat{X}_B). The state after the transformation $U_B(t_2)^{-1}$ is (9), and the measurement of $S_2^{(B)}$ allows an inference of the value of P_A , of system A at time t_2 . The measurement of $S_2^{(B)}$ at B ‘‘collapses’’ system A to either $U_{\pi/8}^{(A)}|\alpha\rangle$ or $U_{\pi/8}^{(A)}|-\alpha\rangle$. Following the method of [68], the inferred statistics is thus given by $U_{\pi/8}^{(A)}|\alpha\rangle$ or $U_{\pi/8}^{(A)}|-\alpha\rangle$, which are superpositions (10) of $|\alpha\rangle$ or $|-\alpha\rangle$, and for which the conditional distributions are $P_+(P_A)$ and $P_-(P_A)$ of eqn (11) respectively. These distributions show fringes, and have the variance $\Delta_{inf}^2 P_A$ for P . This variance of the inferred value for P_A is [64]

$$\Delta_{inf}^2 P_A = \frac{1}{2} - |\alpha|^2 e^{-4|\alpha|^2} \quad (33)$$

The level of combined inference is

$$\varepsilon = \Delta_{inf} X_A \Delta_{inf} P_A < \frac{1}{2} \quad (34)$$

which is below the value for the uncertainty principle, $\Delta X_A \Delta P_A \geq \frac{1}{2}$, thus implying an EPR paradox [68].

It is also known that the observation of (34) demonstrates an EPR steering [71, 73, 74]. If Bell’s premise of *local causality* is assumed valid, the condition (34) is

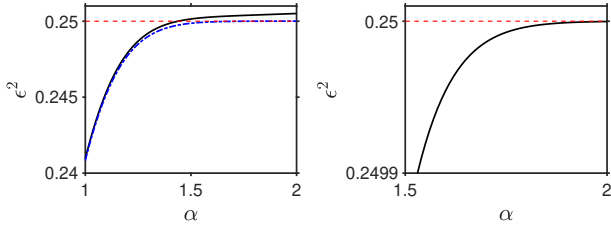


Figure 14. Plots showing the violation of the macroscopic EPR inequality (34). Notation as for Figure 13. Here, we give a close-up of results for the full calculation showing the cut-off values of β needed for $\mathcal{E}^2 < 1/4$, for larger α .

paradoxical because it implies that the system A cannot be specified as being in any mixture of localised *quantum* states φ_+ or φ_- (since such states would need to violate the uncertainty principle) [71, 73, 74]. This negates the hypothesis that the system of (32) can be regarded as being in either $|\alpha\rangle$ or $|- \alpha\rangle$ (or indeed in any φ_+ or φ_- if these are to be quantum states) in a way that is consistent with local causality. The original EPR paradox assumes local realism, a more specific form of local causality useful when one has perfectly correlated results for both conjugate measurements.

In the above prediction for the EPR inequality, it is assumed that an idealised measurement at B “collapses” system A into one or other of the coherent states. In a more rigorous analysis, we evaluate the conditional statistics for system A using the specific proposal for the measurement at B , where the sign of X_B is measured, as in the calculations of Section IV. This gives for the state (8) an inference variance in X_A of

$$\Delta_{inf}^2 X_A = \frac{1}{2} + \frac{2|\alpha|^2}{(1 - e^{-2|\alpha|^2 - 2|\beta|^2})} - \frac{2|\alpha|^2 \operatorname{erf}(\sqrt{2}|\beta|)^2}{(1 - e^{-2|\alpha|^2 - 2|\beta|^2})^2} \quad (35)$$

The full details are given in the Appendix. Similarly, the inferred variance for P is calculated assuming the state (9). We find

$$\Delta_{inf}^2 P_A = \frac{1}{2} + \frac{2|\alpha|^2}{(e^{2|\alpha|^2 + 2|\beta|^2} - 1)} - \frac{|\alpha|^2 \operatorname{erf}(\sqrt{2}|\beta|)^2}{\{e^{2|\alpha|^2} - e^{-2|\beta|^2}\}^2} \quad (36)$$

In the limit of large β , where the measurement becomes ideal, we see that $\Delta^2 X_A \rightarrow 1/2$ and $\Delta^2 P_A$ reduces to (33), consistent with the arguments above. Figures 13 and 14 plot ε^2 for varying β . The results become indistinguishable from the ideal case for larger β .

B. EPR paradox based on weak macroscopic realism

The original EPR paradox argues the incompleteness of quantum mechanics based on the assumption of local

realism, or local causality, as above. As explained in [32], one may also argue an EPR paradox based on the validity of weak macroscopic realism. We summarise this result, for the purpose of comparison.

The cat state for system A is the superposition $c_+|\alpha\rangle + ic_-|-\alpha\rangle$ (for α large), where c_+/c_- is real. Weak macroscopic realism postulates that the system A in such a state is actually in one or other state φ_+ and φ_- for which the value of the macroscopic spin $S_2^{(A)}$ is determined. The spin $S_2^{(A)}$ is measured from the quadrature amplitude X_A (as the sign of X_A). The distribution $P(X_A)$ for X_A gives two distinct Gaussian hills, each hill with variance $(\Delta X_A)^2 = 1/2$ [29]. Following [32], one may specify the variance of X_A for the states φ_+ and φ_- . We denote the specified variances as $(\Delta X_A)_+^2$ and $(\Delta X_A)_-^2$ respectively. With the assumption that φ_+ and φ_- are to be *quantum* states, the Heisenberg uncertainty relation $(\Delta X_A)(\Delta P_A) \geq 1/2$ applies to each state. Then, as explained in [36], for the ensemble of systems in a classical mixture of states φ_+ and φ_- , it is readily proved that $(\Delta X_A)_{ave}(\Delta P_A) \geq 1/2$, where $(\Delta X_A)_{ave}^2 = P_+(\Delta X_A)_+^2 + P_-(\Delta X_A)_-^2$, $P_+ + P_- = 1$ and $P_{\pm} \geq 0$. The violation of

$$\varepsilon_M \equiv (\Delta X_A)_{ave}(\Delta P_A) \geq 1/2 \quad (37)$$

will therefore imply incompatibility of weak macroscopic realism with the completeness of quantum mechanics, since in this case the states φ_+ and φ_- cannot be represented as quantum states. Since here $(\Delta X_A)_{ave} \rightarrow 1/2$ (or more precisely $(\Delta X_A)_{ave} \not\rightarrow 1/2$), we find the inequality (37) is violated for $(\Delta P_A)^2 < 1/2$. This is the case for the Leggett-Garg gedanken experiment, where the distribution $P(P_A)$ at times t_2 and t_3 is given by eqn (11). The variance is [64]

$$(\Delta P_A)^2 = \frac{1}{2} - \alpha^2 e^{-4\alpha^2} \quad (38)$$

The violation is plotted in Figure 13.

C. Discussion

In conclusion, if one assumes weak macroscopic realism (wMR) for the state in a superposition of $|\alpha\rangle$ and $|- \alpha\rangle$, then the fringe distributions shown in Figure 2 do *not* indicate that the system cannot be regarded as having a definite value for the macroscopic spin (as sometimes interpreted). Rather, the fringes signify that those states φ_+ or φ_- which would have definite macroscopic spin values (if defined consistently with wMR) cannot be given as *quantum* states. There is an incompleteness of quantum mechanics, if wMR is to be valid.

The original EPR paradox concluded inconsistency between local realism and the completeness of quantum mechanics [35]. Bell later showed that local realism itself can

be falsified [34]. Similarly, the EPR paradox of Section VI.A shows inconsistency between local causality (at the level of \hbar) and the completeness of quantum mechanics. However, the assumption of local causality itself has been falsified, based on Bell theorems [75, 76], thereby apparently resolving the paradox. By contrast, the EPR-type paradox explained in Section VI.B is not readily resolved in the same manner. This paradox shows inconsistency between wMR and the completeness of quantum mechanics [32]. However, there is to date no obvious way to falsify wMR. The paradox involving weak macroscopic realism is hence different and stronger.

While the present paper studies the EPR paradox associated with a macroscopic superposition state constructed from coherent states, similar EPR paradoxes have been formulated for other types of macroscopic superposition states, e.g for NOON states [77, 78] and Greenberger-Horne-Zeilinger (GHZ) states [64, 79]. However, these paradoxes give inconsistencies for local causality, or local realism. Less has been done on paradoxes that illustrate the inconsistency between weak macroscopic realism and the incompleteness of quantum mechanics, although related examples were given for number-state superpositions in [36]. We expect such paradoxes may also be possible for NOON and GHZ states, and for the higher dimensional GHZ extensions with multiple particles at each site [80, 81].

The method of “irrealism” gives a powerful way to detect the incompleteness of quantum mechanics, along the lines proposed by EPR [82], which could be applied to the examples considered here. In fact, recent work uses irrealism to analyse the incompleteness of the state for the double-slit experiment [83].

VII. CONCLUSION

In this paper, we have illustrated how one may perform delayed-choice experiments using superpositions of two coherent states. We map the original proposals involving spin qubits ($|\uparrow\rangle$ and $|\downarrow\rangle$) onto macroscopic tests, where the qubits are coherent states $|\alpha\rangle$ and $|- \alpha\rangle$ ($\alpha \rightarrow \infty$). The choice of measurement setting corresponds to a choice of a particular unitary interaction. This gives a mapping between the rotations for the spin qubits and those for coherent-state qubits. In order to counter interpretations of the gedanken experiments that would suggest macroscopic retrocausality, we have demonstrated consistency of the predictions with the concept of weak macroscopic realism (wMR).

In Section III, we have presented a version of the delayed-choice quantum eraser experiment, using entangled cat states. The loss of which-way information shows as interference fringes in distributions for the quadrature phase amplitude P . We argued the signature is at the

microscopic level of \hbar (since the fringes must be finely resolved) and hence that there is no evidence of macroscopic retrocausality.

Motivated further, in Sections IV we examined a delayed-choice version of a macroscopic Leggett-Garg test for the entangled cat states. Here, the test explicitly demonstrates failure of macrorealism, thus suggesting an apparent macroscopic retrocausality. The violations of the Leggett-Garg inequalities were then explained by introducing the concept of deterministic macroscopic realism (dMR), which for entangled systems may also be defined as macroscopic local realism. The premise dMR is stricter than that of wMR. We showed that the violations of Leggett-Garg inequalities falsify dMR, but can be viewed consistently with wMR. We thus avoid interpretations of macroscopic retrocausality, by noting the failure of dMR where one has unitary dynamics (in the form of basis rotations that determine the measurement settings), at both sites.

In Section V, the apparent macroscopic retrocausality of the Leggett-Garg set-up is demonstrated in a rigorous way, by showing violation of the dimension witness inequality as in the work of Chaves, Lemos and Pienaar [26]. This implies failure of all two-dimensional non-retrocausal models. One may avoid the conclusion of macroscopic retrocausality, however, because of the higher dimensions evident in the phase-space solutions.

We further showed in Section VI that, although the macroscopic experiments are consistent with weak macroscopic realism (wMR), EPR paradoxes exist for measurements giving a microscopic resolution. The paradoxes indicate incompatibility between local causality (and wMR) with the completeness of quantum mechanics. The latter is a strong paradox, because wMR has not yet been falsified.

It is interesting to consider the prospect of an experiment. The two-mode entangled cat states have been generated [37, 84, 85]. The significant challenge is to realise the unitary rotation, which is given by the Hamiltonian $H_{NL} = \Omega \hat{n}^4$ with a quartic dependence on the field boson number. The quantum eraser can be carried out more straightforwardly, using the interaction $H_{NL} = \Omega \hat{n}^2$, which has been experimentally achieved as a Kerr nonlinearity [38, 39]. Realisations may also be possible using mesoscopic NOON states and the nonlinear N -scopic beam splitter interaction for N bosons, described in [31].

ACKNOWLEDGEMENTS

This research has been supported by the Australian Research Council Discovery Project Grants schemes under Grant DP180102470.

APPENDIX

A. Quantum eraser and EPR calculation

Here, we give details for the superposition $U_{\pi/8}|\pm\alpha\rangle = e^{-i\pi/8}\{\cos\pi/8|\pm\alpha\rangle + i\sin\pi/8|\mp\alpha\rangle\}$ examined in Section III. The calculations for the superposition $U_{\pi/4}|\pm\alpha\rangle$ are similar.

It is straightforward to evaluate $P(P_A)_+ = |\langle P_A|U_{\pi/8}|\alpha\rangle|^2$ and $P(P_A)_- = |\langle P_A|U_{\pi/8}|-\alpha\rangle|^2$ for the simple case. For the accurate calculation based on the actual measurements that would be used, one considers $|\psi(t_4)\rangle$ and evaluates $P(P_A, X_B) = |\langle X_B|\langle P_A|\psi(t_4)\rangle|^2$

$$P(P_A, X_B) = 2 \frac{\exp(-P_A^2 - X_B^2 - 2|\beta|^2)}{\pi(1 - e^{-2|\alpha|^2 - 2|\beta|^2})} \left\{ \sin^2(\sqrt{2}P_A|\alpha|) + \sinh^2(\sqrt{2}X_B|\beta|) - \frac{\sqrt{2}}{4} \sin(2\sqrt{2}P_A|\alpha|) \sinh(2\sqrt{2}X_B|\beta|) \right\} \quad (39)$$

This gives the result (12) using $P(P_A)_\pm = P(P_A|X_B \gtrless 0)$ and

$$P(X_B) = \int P(P_A, X_B) dP_A = \frac{\exp(-X_B^2 - 2|\beta|^2)}{\sqrt{\pi}(1 - e^{-2|\alpha|^2 - 2|\beta|^2})} \left(1 - e^{-2|\alpha|^2} + 2 \sinh^2(\sqrt{2}X_B|\beta|) \right) \quad (40)$$

To evaluate the EPR correlations, we calculate the variance of $P(P_A)_\pm$. We find for the simple analysis

$$\begin{aligned} \int P_A P(P_A)_\pm dP_A &= \frac{1}{\pi^{1/2}} \left\{ \int P_A e^{-P_A^2} dP_A \mp \frac{1}{\sqrt{2}} \int P_A e^{-P_A^2} \sin(2\sqrt{2}P_A|\alpha|) dP_A \right\} \\ &= \frac{1}{\pi^{1/2}} \left\{ 0 \mp \frac{1}{\sqrt{2}} \sqrt{2} \sqrt{\pi} |\alpha| e^{-2|\alpha|^2} \right\} = \mp |\alpha| e^{-2|\alpha|^2} \\ \int P_A^2 P(P_A)_\pm dP_A &= \frac{1}{\pi^{1/2}} \left\{ \int P_A^2 e^{-P_A^2} dP_A \mp \frac{1}{\sqrt{2}} \int P_A^2 e^{-P_A^2} \sin(2\sqrt{2}P_A|\alpha|) dP_A \right\} \\ &= \frac{1}{\pi^{1/2}} \left\{ \frac{\sqrt{\pi}}{2} \mp 0 \right\} = \frac{1}{2} \end{aligned} \quad (41)$$

which gives the result (33). For the complete measurement, we use the full result (12) for $P(P_A)_\pm$. Integration gives

$$\begin{aligned} \int P_A P(P_A)_\pm dP_A &= \mp \frac{|\alpha| \operatorname{erf}(\sqrt{2}|\beta|)}{\{e^{2|\alpha|^2} - e^{-2|\beta|^2}\}} \\ \int P_A^2 P(P_A)_\pm dP_A &= \frac{1}{2} + \frac{2|\alpha|^2}{(e^{2|\alpha|^2 + 2|\beta|^2} - 1)} \end{aligned} \quad (42)$$

leading to (36).

B. Calculation of EPR correlations

We first evaluate $\Delta_{inf}^2 X_A$ for the state (8). The inferred variance is defined as

$$\Delta_{inf}^2 X_A = P(X_B > 0) \Delta_+^2 X_A + P(X_B \leq 0) \Delta_-^2 X_A \quad (43)$$

where clearly $P(X_B > 0) = 1/2$. The conditional distributions are defined

$$P_+(X_A) = P(X_A|X_B > 0) = \frac{\int_0^\infty P(X_A, X_B) dX_B}{\int_0^\infty P(X_B) dX_B} \quad (44)$$

and similarly $P_-(X_A) = P(X_A|X_B \leq 0)$, which, after evaluation of $P(X_A, X_B)$ for the entangled cat state, gives

$$P(X_A)_\pm = \frac{2\mathcal{N}^2 e^{-X_A^2 - 2|\alpha|^2}}{\sqrt{\pi}} \left\{ \cosh(2\sqrt{2}|\alpha|X_A) \mp \operatorname{erf}(\sqrt{2}|\beta|) \sinh(2\sqrt{2}|\alpha|X_A) - e^{-2|\beta|^2} \right\} \quad (45)$$

The variance of these distributions are $\Delta_{\pm}^2 \hat{X}_A = \langle \hat{X}_A^2 \rangle - \langle \hat{X}_A \rangle^2$ where

$$\begin{aligned} \langle \hat{X}_A \rangle_{\pm} &= \int P_{\pm}(X_A) X_A dX_A = \frac{\mp \sqrt{2} |\alpha| \operatorname{erf}(\sqrt{2} |\beta|)}{(1 - e^{-2|\alpha|^2 - 2|\beta|^2})} \\ \langle \hat{X}_A^2 \rangle_{\pm} &= \int P_{\pm}(X_A) X_A^2 dX_A = \frac{1}{2} + \frac{2|\alpha|^2}{(1 - e^{-2|\alpha|^2 - 2|\beta|^2})} \end{aligned} \quad (46)$$

This leads to the result

$$\begin{aligned} \Delta_{inf}^2 X_A &= \frac{1}{2} + 4\mathcal{N}^2 |\alpha|^2 - 8\mathcal{N}^4 |\alpha|^2 \operatorname{erf}(\sqrt{2} |\beta|)^2 \\ &= \frac{1}{2} + \frac{2|\alpha|^2}{(1 - e^{-2|\alpha|^2 - 2|\beta|^2})} - \frac{2|\alpha|^2 \operatorname{erf}(\sqrt{2} |\beta|)^2}{(1 - e^{-2|\alpha|^2 - 2|\beta|^2})^2} \end{aligned} \quad (47)$$

Similarly, we evaluate $\Delta_{inf}^2 P_A$ for the state (9). Here,

$$\Delta_{inf}^2 P_A = P(X_B > 0) \Delta_+^2 P_A + P(X_B \leq 0) \Delta_-^2 P_A$$

We first evaluate evaluate the conditional distributions of

$$P_+(P_A) = P(P_A | X_B > 0) = \frac{\int_0^{\infty} P(P_A, X_B) dX_B}{\int_0^{\infty} P(X_B) dX_B} \quad (48)$$

and similarly, $P_-(P_A) = P(P_A | X_B \leq 0) = \frac{\int_{-\infty}^0 P(P_A, X_B) dX_B}{\int_{-\infty}^0 P(X_B) dX_B}$ using

$$\begin{aligned} P(P_A, X_B) &= |\langle X_B | \langle P_A | \psi(t_4) \rangle|^2 \\ &= \frac{e^{-P_A^2}}{\sqrt{\pi} \{1 - e^{-2|\alpha|^2 - 2|\beta|^2}\}} \left\{ 1 - e^{-2|\beta|^2} \cos(2\sqrt{2} P_A |\alpha|) - \frac{\sqrt{2}}{2} \operatorname{erf}(\sqrt{2} |\beta|) \sin(2\sqrt{2} P_A |\alpha|) \right\} \end{aligned} \quad (49)$$

This gives

$$P_{\pm}(P_A) = \frac{2\mathcal{N}^2 e^{-P_A^2}}{\sqrt{\pi}} \left\{ 1 - e^{-2|\beta|^2} \cos(2\sqrt{2} P_A |\alpha|) \mp \frac{\sqrt{2}}{2} \operatorname{erf}(\sqrt{2} |\beta|) \sin(2\sqrt{2} P_A |\alpha|) \right\} \quad (50)$$

Hence

$$\begin{aligned} \langle \hat{P}_A \rangle_{\pm} &= \int P_{\pm}(P_A) P_A dP_A = \mp \frac{|\alpha| e^{-2|\alpha|^2} \operatorname{erf}(\sqrt{2} |\beta|)}{\{1 - e^{-2|\alpha|^2 - 2|\beta|^2}\}} \\ \langle \hat{P}_A^2 \rangle_{\pm} &= \int P_{\pm}(P_A) P_A^2 dP_A = \frac{1}{2} + \frac{2|\alpha|^2}{\{e^{2|\alpha|^2 + 2|\beta|^2} - 1\}} \end{aligned} \quad (51)$$

which leads to

$$\begin{aligned} \Delta_{inf}^2 P_A &= \frac{1}{2} + 4\mathcal{N}^2 |\alpha|^2 e^{-2|\alpha|^2 - 2|\beta|^2} - 4\mathcal{N}^4 |\alpha|^2 e^{-4|\alpha|^2} \operatorname{erf}(\sqrt{2} |\beta|)^2 \\ &= \frac{1}{2} + \frac{2|\alpha|^2 e^{-2|\alpha|^2 - 2|\beta|^2}}{\{1 - e^{-2|\alpha|^2 - 2|\beta|^2}\}} - \frac{|\alpha|^2 e^{-4|\alpha|^2} \operatorname{erf}(\sqrt{2} |\beta|)^2}{\{1 - e^{-2|\alpha|^2 - 2|\beta|^2}\}^2} \end{aligned} \quad (52)$$

C. Cat state dynamics for the Dimension Witness test

In this section we consider the two state solution for our dynamically evolved macroscopic cat states under a non-linear interaction. Considering α to be real, for an initial coherent state $|\alpha\rangle$ undergoing an evolution with a non-linear interaction H_{NL} , the state created after an interaction time t_{θ} can be written as,

$$|\alpha, t_\theta\rangle = \exp\left[-\frac{|\alpha|^2}{2}\right] \sum_{n=0}^{\infty} \alpha^n \frac{\exp(-i\Omega t_\theta n^k)}{\sqrt{n!}} |n\rangle \quad (53)$$

We restrict to $k = 4$. Let us constrain to $t_\theta = m\pi/8$ where m is an integer and choose the units of time such that $\Omega = 1$. To obtain the two-state solution in terms of $|\alpha\rangle$ and $|-\alpha\rangle$, we require solutions of type

$$\exp\left[-\frac{|\alpha|^2}{2}\right] \sum_n \alpha^n \frac{\exp(-im\frac{\pi}{8}n^4)}{\sqrt{n!}} |n\rangle = \exp\left[-\frac{|\alpha|^2}{2}\right] \sum_n A \frac{\alpha^n}{\sqrt{n!}} |n\rangle + \exp\left[-\frac{|\alpha|^2}{2}\right] \sum_n B \frac{(-1)^n \alpha^n}{\sqrt{n!}} |n\rangle \quad (54)$$

where A and B are constants. Now since the summation indexes are the same, this requires $\exp(-im\frac{\pi}{8}n^4) = A + (-1)^n B$. By assigning $n = 0, 1$ we find $A + B = 1$ and $e^{-im\frac{\pi}{8}} = A - B$, giving the solutions as

$$\begin{aligned} A &= e^{-im\frac{\pi}{16}} \cos\left(m\frac{\pi}{16}\right) \\ B &= ie^{-im\frac{\pi}{16}} \sin\left(m\frac{\pi}{16}\right) \end{aligned} \quad (55)$$

Hence we propose that for all integers n such that $n = 0, 1, 2, \dots$

$$\exp\left(-im\frac{\pi}{8}n^4\right) = e^{-im\frac{\pi}{16}} \left(\cos\left(m\frac{\pi}{16}\right) + (-1)^n i \sin\left(m\frac{\pi}{16}\right) \right) \quad (56)$$

We now prove this to be true. For even n , we see that the right side of equation (56) satisfies $RHS = 1$. We can write $n = 2J$ where $J = 1, 2, \dots$ in which case $n^4 = (2J)^4 = 16J^4$. Then we see that the left side (LHS) of equation (56) satisfies $LHS = 1$, since m is an integer. Next we consider odd n . We see that $RHS = e^{-im\frac{\pi}{8}}$. We can write $n = 2J + 1$, where J is an integer, $J \geq 1$. We now show that $n^4 = (2J + 1)^4 = 16M + 1$, where M is integer. This is proved by considering $(2J + 1)^4 = 16J^4 + 32J^3 + 24J^2 + 8J + 1$ from which we see that the condition holds if J is even. Then also, $(2J + 1)^4 - 1 = 16\{J^4 + 2J^3 + \frac{J}{2}(3J + 1)\}$. This gives the result, since $3J + 1$ is even if J is odd and the term $\{J^4 + 2J^3 + \frac{J}{2}(3J + 1)\}$ becomes an integer for all values of J . Hence, $LHS = \exp(-im\frac{\pi}{8})$. Hence we can write a two state solution for time multiples of $\pi/8$, as

$$|\alpha, t_\theta\rangle = e^{-it_\theta/2} (\cos(t_\theta/2) |\alpha\rangle + i \sin(t_\theta/2) |-\alpha\rangle) \quad (57)$$

where $t_\theta = m\frac{\pi}{8}$.

-
- [1] J. A. Wheeler, "The 'past' and the 'delayed-choice' double-slit experiment," in *Mathematical Foundations of Quantum Theory*, edited by A. R. Marlow (Academic Press, New York, 1978) pp. 9–48.
- [2] J. A. Wheeler in "Quantum Theory and Measurement" by J. A. Wheeler and W. H. Zurek (Princeton University Press pp. 192–213, 1984).
- [3] Xi. Ma, J. Kofler, and A. Zeilinger, "Delayed-choice gedanken experiments and their realizations", *Rev. Mod. Phys.* **88**, 015005 (2016) and references therein.
- [4] M. O. Scully and K. Drühl, Quantum eraser: A proposed photon correlation experiment concerning observation and 'delayed choice' in quantum mechanics, *Phys. Rev. A* **25**, 2208 (1982).
- [5] M. O. Scully, B.-G. Englert, and H. Walther, Quantum optical tests of complementarity, *Nature (London)* **351**, 111 (1991).

-
- [6] T. J. Herzog, P. G. Kwiat, H. Weinfurter, and A. Zeilinger, Complementarity and the quantum eraser, *Phys. Rev. Lett.* **75**, 3034 (1995).
- [7] Y.-H. Kim, R. Yu, S. P. Kulik, Y. Shih, and M. O. Scully, Delayed choice quantum eraser, *Phys. Rev. Lett.* **84**, 1 (2000).
- [8] S. P. Walborn, M. O. Terra Cunha, S. Pádua, and C. H. Monken, Double-Slit Quantum Eraser, *Phys. Rev. A* **65**, 033818 (2002).
- [9] V. Jacques, E. Wu, F. Grosshans, F. Treussart, P. Grangier, A. Aspect, and J.-F. Roch, "Experimental realization of wheelers delayed-choice gedanken experiment". *Science* **315**, 5814 (2007).
- [10] A. G. Manning, R. I. Khakimov, R. G. Dall, and A. G. Truscott, "Wheeler's delayed-choice gedanken experiment with a single atom". *Nat. Phys.* **11**, 539–542 (2015).
- [11] J.-S. Tang, Y.-L. Li, X.-Y. Xu, G.-Y. Xiang, C.-F. Li, and G.-C. Guo, Realization of quantum Wheelers delayed-choice experiment, *Nat. Photon.* **6**, 600 (2012).
- [12] Xiao-Song Ma et al., Quantum erasure with causally dis-

- connected choice, *Proceedings of the National Academy of Sciences* **110** (4) (2013).
- [13] B. G. Englert, M. O. Scully, and H. Walther, Quantum erasure in double-slit interferometers with which-way detectors, *Am. J. Phys.* **67**, 325 (1999).
- [14] U. Mohrhoff, Objectivity, retrocausation, and the experiment of Englert, Scully, and Walther, *Am. J. Phys.* **67**, 330 (1999).
- [15] R. E. Kastner, The ‘delayed choice quantum eraser’ neither erases nor delays,” *Found. Phys.* **49**, 717 (2019).
- [16] R. L. Ingraham, Quantum nonlocality in a delayed-choice experiment with partial, controllable memory erasing, *Phys. Rev. A* **50**, 4502 (1994). R. L. Ingraham, “Erratum: *Phys. Rev. A* **51**, 4295 (1995).
- [17] S. Faetti, “An alternative analysis of the delayed-choice quantum eraser”, arXiv:1912.04101 [quant-ph].
- [18] Brian R. La Cour and Thomas W. Yudichak, Classical model of delayed-choice quantum eraser, *Phys. Rev. A* **103**, 062213 (2021).
- [19] R. Ionicioiu and D. Terno, Proposal for a quantum delayed-choice experiment, *Phys. Rev. Lett.* **107**, 230406 (2011).
- [20] R. Ionicioiu, T. Jennewein, R. B. Mann, and D. R. Terno, Is wave-particle objectivity compatible with determinism and locality?, *Nat. Commun.* **5**, 4997 (2014).
- [21] R. Rossi, Restrictions for the causal inferences in an interferometric system, *Phys. Rev. A* **96**, 012106 (2017).
- [22] A. S. Rab, E. Polino, Z.-X. Man, N. Ba An, Y.-J. Xia, N. Spagnolo, R. Lo Franco, and F. Sciarrino, Entanglement of photons in their dual wave-particle nature, *Nat. Commun.* **8**, 915 (2017).
- [23] A. Peruzzo, P. Shadbolt, N. Brunner, S. Popescu and J. L. O’Brien. A Quantum Delayed-Choice Experiment, *Science* **338**, 634 (2012).
- [24] F. Kaiser, T. Coudreau, P. Milman, D. B. Ostrowsky, and S. Tanzilli, Entanglement-enabled delayed-choice experiment. *Science* **338**, 637 (2012).
- [25] S. B. Zheng, Y. P. Zhong, K. Xu, Q. J. Wang, H. Wang, L. T. Shen, C. P. Yang, J. M. Martinis, A. N. Cleland, and S. Y. Han, Quantum delayed-choice experiment with a beam splitter in a quantum superposition, *Phys. Rev. Lett.* **115**, 260403 (2015).
- [26] R. Chaves, G. B. Lemos and J. Pienaar, Causal Modeling the Delayed-Choice Experiment, *Phys. Rev. Lett.* **120**, 190401 (2018).
- [27] E. Polino, I. Agresti, D. Poderini, G. Carvacho, G. Milani, G. B. Lemos, R. Chaves and F. Sciarrino, Device-independent test of a delayed choice experiment, *Phys. Rev. A* **100**, 022111 (2019).
- [28] H.-L. Huang, Y.-H. Luo, B. Bai, Y.-H. Deng, H. Wang, Q. Zhao, H.-S. Zhong, Y.-Q. Nie, W.-H. Jiang, X.-L. Wang et al., Compatibility of causal hidden-variable theories with a delayed-choice experiment, *Phys. Rev. A* **100**, 012114 (2019).
- [29] B. Yurke and D. Stoler, Generating quantum mechanical superpositions of macroscopically distinguishable states via amplitude dispersion, *Phys. Rev. Lett.* **57**, 13 (1986).
- [30] M. Thenabadu and M. D. Reid, Leggett-Garg tests of macrorealism for dynamical cat states evolving in a nonlinear medium, *Phys. Rev. A* **99**, 032125 (2019).
- [31] M. Thenabadu, G.-L. Cheng, T. L. H. Pham, L. V. Drummond, L. Rosales-Zárata and M. D. Reid, Testing macroscopic local realism using local nonlinear dynamics and time settings, *Phys. Rev. A* **102**, 022202 (2020).
- [32] M. Thenabadu and M. D. Reid, Bipartite Leggett-Garg and macroscopic Bell inequality violations using cat states: distinguishing weak and deterministic macroscopic realism arXiv:2012.14997; MD Reid and M Thenabadu, Weak versus deterministic macroscopic realism, arXiv:2101.09476
- [33] A. Leggett and A. Garg, Quantum mechanics versus macroscopic realism: is the flux there when nobody looks? *Phys. Rev. Lett.* **54**, 857 (1985).
- [34] J. S. Bell, On the Einstein-Podolsky-Rosen paradox, *Physics* **1**, 195 (1964).
- [35] A. Einstein, B. Podolsky, and N. Rosen, Can Quantum-Mechanical Description of Physical Reality Be Considered Complete?, *Phys. Rev.* **47**, 777 (1935).
- [36] M. D. Reid, Criteria to detect macroscopic quantum coherence, macroscopic quantum entanglement, and an Einstein-Podolsky-Rosen paradox for macroscopic superposition states, *Phys. Rev. A* **100**, 052118 (2019).
- [37] C. Wang et al., A Schrödinger cat living in two boxes, *Science* **352**, 1087 (2016).
- [38] M. Greiner, O. Mandel, T. Hänsch and I. Bloch, Collapse and revival of the matter wave field of a Bose-Einstein condensate, *Nature* **419**, 51 (2002).
- [39] G. Kirchmair et al., Observation of the quantum state collapse and revival due to a single-photon Kerr effect, *Nature* **495**, 205 (2013).
- [40] N. S. Williams and A. N. Jordan, Weak Values and the Leggett-Garg Inequality in Solid-State Qubits, *Phys. Rev. Lett.* **100**, 026804 (2008).
- [41] A. N. Jordan, A. N. Korotkov, and M. Buttiker, Leggett-Garg Inequality with a Kicked Quantum Pump, *Phys. Rev. Lett.* **97**, 026805 (2006).
- [42] L. Clemente and J. Kofler, Necessary and sufficient conditions for macroscopic realism from quantum mechanics, *Phys. Rev. A* **91**, 062103 (2015).
- [43] J. J. Halliwell and C. Mawby, Conditions for Macrorealism for Systems Described by Many-Valued Variables, *Phys. Rev. A* **102**, 012209 (2020).
- [44] J. P. Dowling, Quantum optical metrology – the low-down on high-NOON states, *Contemporary Physics* **49**, 125 (2008).
- [45] B. Opanchuk, L. Rosales-Zárata, R. Y Teh, and M. D. Reid, Quantifying the mesoscopic quantum coherence of approximate NOON states and spin-squeezed two-mode Bose-Einstein condensates, *Phys. Rev. A* **94**, 062125 (2016).
- [46] C. Emary, N. Lambert, and F. Nori, Leggett-Garg inequalities, *Rep. Prog. Phys.* **77**, 016001 (2014).
- [47] G. C. Knee, K. Kakuyanagi, M.-C. Yeh, Y. Matsuzaki, H. Toida, H. Yamaguchi, S. Saito, A. J. Leggett and W. J. Munro, A strict experimental test of macroscopic realism in a superconducting flux qubit, *Nat. Commun.* **7**, 13253 (2016).
- [48] A. Palacios-Laloy, F. Mallet, F. Nguyen, P. Bertet, Denis Vion, Daniel Esteve and Alexander N. Korotkov, Experimental violation of a Bell’s inequality in time with weak measurement, *Nature Phys.* **6**, 442 (2010).
- [49] J. Dressel and A. N. Korotkov, Avoiding loopholes with hybrid bell-leggett-garg inequalities, *Phys. Rev. A* **89**, 012125 (2014).
- [50] J. Dressel, C. J. Broadbent, J. C. Howell and A. N. Jordan, Experimental Violation of Two-Party Leggett-Garg Inequalities with Semiweak Measurements, *Phys. Rev. Lett.* **106**, 040402 (2011).

- [51] M. E. Goggin, et al., Violation of the Leggett-Garg inequality with weak measurements of photons, *Proc. Natl. Acad. Sci.* **108**, 1256 (2011).
- [52] A. Asadian, C. Brukner, and P. Rabl, Probing Macroscopic Realism via Ramsey Correlation Measurements, *Phys. Rev. Lett.* **112**, 190402 (2014).
- [53] C. Budroni, G. Vitagliano, G. Colangelo, R. J. Sewell, O. Gühne, G. Tóth, and M. W. Mitchell, Quantum Non-demolition Measurement Enables Macroscopic Leggett-Garg Tests, *Phys. Rev. Lett.* **115**, 200403 (2015).
- [54] L. Rosales-Zárate, B. Opanchuk, Q. Y. He, and M. D. Reid, Leggett-Garg tests of macrorealism for bosonic systems including two-well Bose-Einstein condensates and atom interferometers, *Phys. Rev. A* **97**, 042114 (2018).
- [55] R. Uola, G. Vitagliano and C. Budroni, Leggett-Garg macrorealism and the quantum nondisturbance conditions, *Phys. Rev. A* **100**, 042117 (2019).
- [56] J. Halliwell, A. Bhatnagar, E. Ireland, H. Nadeem and V. Wimalaweera, Leggett-Garg tests for macrorealism: interference experiments and the simple harmonic oscillator, *Phys. Rev. A* **103**, 032218 (2021).
- [57] A. K. Pan, “Interference experiment, anomalous weak value, and Leggett-Garg test of macrorealism”, *Phys. Rev. A* **102**, 032206 (2020).
- [58] N. Brunner, S. Pironio, A. Acín, N. Gisin, A. A. Méthot and V. Scarani, “Testing the Dimension of Hilbert Spaces”, *Phys. Rev. Lett.* **100**, 210503 (2008).
- [59] R. Gallego, N. Brunner, C. Hadley and A. Acín, “Device-Independent Tests of Classical and Quantum Dimensions”, *Phys. Rev. Lett.* **105**, 230501 (2010).
- [60] J. Bowles, M. T. Quintino, and N. Brunner, Certifying the Dimension of Classical and Quantum Systems in a Prepare-and-Measure Scenario with Independent Devices, *Phys. Rev. Lett.* **112**, 140407 (2014).
- [61] J. Ahrens, P. Badzi, A. Cabello, and M. Bourennane, Experimental device-independent tests of classical and quantum dimensions, *Nat. Phys.* **8**, 592 (2012).
- [62] S. Yu, Y.N. Sun, W. Liu, Z.D. Liu, Z.J. Ke, Y.T. Wang, J.S. Tang, C.F. Li, and G.C. Guo, Realization of a causal-modeled delayed-choice experiment using single photons, *Phys. Rev. A* **100**, 012115 (2019).
- [63] L. Rosales-Zarate, R. Y. Teh, S. Kiesewetter, A. Brolis, K. Ng, and M. D. Reid, Decoherence of Einstein-Podolsky-Rosen steering, *J. Opt. Soc. Am. B* **32** A82 (2015).
- [64] M. D. Reid, Interpreting the macroscopic pointer by analysing the elements of reality of Schrodinger cat, *J. Phys. A: Math. Theor.* **50**, 41LT01 (2017).
- [65] M. Brune, E. Hagley, J. Dreyer, X. Maître, A. Maali, C. Wunderlich, J. M. Raimond, and S. Haroche, Observing the Progressive Decoherence of the “Meter” in a Quantum Measurement, *Phys. Rev. Lett.* **77**, 4887 (1996).
- [66] C. Monroe, D. M. Meekhof, B. E. King, D. J. Wineland, A “Schrodinger cat” superposition state of an atom, *Science* **272**, 1131 (1996).
- [67] F. Fröwis, P. Sekatski, W. Dür, N. Gisin, and N. Sangouard, Macroscopic quantum states: measures, fragility, and implementations, *Rev. Mod. Phys.* **90**, 025004 (2018).
- [68] M. D. Reid, Demonstration of the Einstein-Podolsky-Rosen Paradox using Nondegenerate Parametric Amplification, *Phys. Rev. A* **40**, 913 (1989).
- [69] M. D. Reid, P. D. Drummond, W. P. Bowen, E. G. Cavalcanti, P. K. Lam, H. A. Bachor, U. L. Andersen and G. Leuchs, The Einstein-Podolsky-Rosen paradox: From concepts to applications, *Rev. Mod. Phys.* **81**, 1727 (2009).
- [70] E. G. Cavalcanti, P. D. Drummond, H. A. Bachor and M. D. Reid, Spin entanglement, decoherence and Bohm’s EPR paradox, *Optics Express* **17** (21), 18693 (2009).
- [71] H. M. Wiseman, S. J. Jones and A. C. Doherty, Steering, Entanglement, Nonlocality and the Einstein-Podolsky-Rosen Paradox, *Phys. Rev. Lett.* **98**, 140402 (2007).
- [72] S. J. Jones, H. M. Wiseman and A. Doherty, Entanglement, Einstein-Podolsky-Rosen correlations, Bell nonlocality, and steering, *Phys. Rev. A* **76**, 052116 (2007).
- [73] E. G. Cavalcanti, S. J. Jones, H. M. Wiseman and M. D. Reid, Experimental criteria for steering and the Einstein-Podolsky-Rosen paradox, *Phys. Rev. A* **80**, 032112 (2009).
- [74] R. Uola, A. C. S. Costa, H. C. Nguyen, and O. Gühne, Quantum Steering, *Rev. Mod. Phys.* **92**, 015001 (2020).
- [75] J. Clauser and A. Shimony, Bell’s theorem: experimental tests and implications, *Rep. Prog. Phys.* **41**, 1881 (1978).
- [76] Nicolas Brunner, Daniel Cavalcanti, Stefano Pironio, Valerio Scarani and Stephanie Wehner, Bell nonlocality, *Rev. Mod. Phys.* **86**, 419 (2014).
- [77] R. Y. Teh, L. Rosales-Zárate, B. Opanchuk, and M. D. Reid, Signifying the nonlocality of NOON states using Einstein-Podolsky-Rosen steering inequalities, *Phys. Rev. A* **94**, 042119 (2016).
- [78] S. Slussarenko, Morgan M. Weston, Helen M. Chrzanowski, Lynden K. Shalm, Varun B. Verma, Sae Woo Nam & Geoff J. Pryde, Unconditional violation of the shot-noise limit in photonic quantum metrology, *Nature Photonics* **11**, 700 (2017).
- [79] D. M. Greenberger, M. A. Horne and A. Zeilinger, in “Bell’s Theorem, Quantum Theory, and Conceptions of the Universe” (Kluwer, Dordrecht, 1989), p. 69.
- [80] M. D. Reid and W. J. Munro, Macroscopic boson states exhibiting the Greenberger-Horne-Zeilinger contradiction with local realism, *Phys. Rev. Lett.* **69**, 997 (1992).
- [81] W. Son, Jinhyoung Lee, and M. S. Kim, Generic Bell Inequalities for Multipartite Arbitrary Dimensional Systems, *Phys. Rev. Lett.* **96**, 060406 (2006).
- [82] A. L. O. Bilobran and R. M. Angelo, A measure of physical reality, *Europhys. Lett.* **112**, 40005 (2015).
- [83] F. R. Lustosa, P. R. Dieguez, and I. G. da Paz, Irrealism from fringe visibility in matter waves double-slit interference with initial contractive states, *Phys. Rev. A* **102**, 052205 (2020).
- [84] P. Milman, A. Auffeves, F. Yamaguchi, M. Brune, J. M. Raimond, and S. Haroche, A proposal to test Bell’s inequalities with mesoscopic non-local states in cavity qed, *Eur. Phys. J. D* **32**, 233 (2005).
- [85] Z. Leghtas, G. Kirchmair, B. Vlastakis, M. H. Devoret, R. J. Schoelkopf, and M. Mirrahimi, Deterministic protocol for mapping a qubit to coherent state superpositions in a cavity, *Phys. Rev. A* **87**, 042315 (2013).